PURDUE UNIVERSITY
GRADUATE SCHOOL
Thesis/Dissertation Acceptance

This is to certify that the thesis/dissertation prepared

By <u>Vinay Kumar Suryadevara</u>

Entitled
LOW POWER STEERING ELECTRODES WITHIN MICROFLUIDIC CHANNELS FOR BLOOD CANCER CELL
SEPARATION FOR MRD APPLICATIONS

For the degree of <u>Master of Science in Electrical and Computer Engineering</u>

Is approved by the final examining committee:

Dr. Maher Rizkalla
Chair

Dr. Sherif S Farag
Co-chair

Dr. Paul Salama
Co-chair

To the best of my knowledge and as understood by the student in the Thesis/Dissertation
Agreement, Publication Delay, and Certification Disclaimer (Graduate School Form 32),
this thesis/dissertation adheres to the provisions of Purdue University's "Policy of
Integrity in Research" and the use of copyright material.

Approved by Major Professor(s): Dr. Maher Rizkalla

Approved by: Dr. Paul Salama   10/05/2015

Head of the Departmental Graduate Program   Date

LOW POWER STEERING ELECTRODES WITHIN MICROFLUIDIC

CHANNELS FOR BLOOD CANCER CELL SEPARATION FOR MRD

APPLICATIONS

A Thesis

Submitted to the Faculty

of

Purdue University

by

Suryadevara Vinay Kumar

In Partial Fulfillment of the

Requirements for the Degree

of

Master of Science in Electrical and Computer Engineering

December 2015

Purdue University

Indianapolis, Indiana

ACKNOWLEDGMENTS

TABLE OF CONTENTS

LIST OF TABLES

LIST OF FIGURES

SYMBOLS

m_p	Mass of the particle
v_f	Velocity of the fluid
v_p	Velocity of the particle
$f0$	Frequency of the electric field
r_p	Radius of the particle
R_i	Inner radius of the cell
R_o	Outer radius of the cell
R_e	Reynolds number
Fe	Iron
F_{ext}	Total force on a particle
F_{Dep}	Total dielectrophoretic force on a particle
E_{rms}	Total electric field
$sigma_{eff}$	Omic conductivity
g_m	Transmembrane conductance
c_m	Surface capacitance
$omega$	Angular frequency
$sigma\_f$	Fluid medium conductivity
$epsilon\_f$	Fluid relative permittivity
$epsilon\_f^*$	Complex fluid relative permittivity
$epsilon\_eq$	Equivalent relative permittivity
rho_f	Fluid density
mu_f	Fluid dynamic viscosity
rho_p	Particle density (RBCs and platelets)
dp	Particle diameter

sigma_p	Particle conductivity
epsilon_p	Particle relative permittivity
epsilon_p*	Complex particle relative permittivity
sigma_s	Shell electrical conductivity
epsilon_s	Shell relative permittivity
th_s	Shell thickness

ABBREVIATIONS

AC	Alternating current
CTC	Cancer tumor cells
CBC	Cancer blood cells
CLIA	Clinical laboratory improvement amendments
DNA	Deoxyribonucleic acid
DC	Direct current
EDL	Electric double layer
LOC	Lab on chip
MRD	Minimal residual disease
MEMS	Micro-electro-mechanical systems
NEMS	Nano-electro-mechanical systems
PMMA	Para-Methoxymethamphetamine
PDMS	Polydimethylsiloxane
3D	Three dimensional
SOC	System on chip

ABSTRACT

Suryadevara, Vinay Kumar. M.S.E.C.E., Purdue University, December 2015. Low Power Steering Electrodes Within Microfluidic Channels For Blood Cancer Cell Separation for MRD Applications. Major Professor: Dr. Maher Rizkalla.

In this study, a novel model for manipulating cancer blood cells based on multi-stage micro channels under varied low field concepts is proposed. Steering Device approach was followed to manipulate the cancer cells based on their various differential potentials across their membranes.

The proposed approach considers the size and the surface potential as well as the iso electronic structure of the cells. This research objectives emphasize the separation of the cells in the blood stream, and differentiate various blood cells and tumors for further analysis within the microfluidic channels. The dimensions of the channel sets the required electric field for manipulating the cancer cells within the channels using low electrode voltage function. The outcomes of this research may introduce a new diagnostic approach of finding the minimum residual disease (MRD) scans, early detection and analysis scans.

This thesis provides a mathematical model, detailing the theory of the cell sorting device, manipulating the blood cancer cells and design of the device structure are also detailed, leading to the optimum research parameters and process. A Computer Aided Design (CAD) was used to model the multi-cell sorting lab-on-chip device, details of hardware and software used in the simulation of the device various stages. Reverse engineering to configure the potentials for sorting mechanism needs is discussed. The thesis work also presents a comparative study of this sorting mechanism and the other commercially available devices. The practical model of the proposed research is laid out for future consideration.

1. INTRODUCTION

Microfluidics systems are those that combine very small size fluid channels with the state-of-the-art micro and nano devices and processes, leading to novel manufacturing systems. Microfluidic systems have diverse potential applications in particular as applied to the medical and pharmaceutical field, including blood-cell-separation equipment, drug screening and delivery, and electrochromatography, among others. Recent developments cover system on chip (SOC), Lab on Chip (LOC), non-invasive sensors, micro-electro-mechanical systems (MEMS), and nanoelectromechanical systems (NEMS). These devices have gained significant commercial applications in recent years [1], [2].

Since the emphasis of this work is cell sorting mechanisms, separating the cancer blood cells from the normal cells, we will focus in this section on application of the microfluidic systems in cell sorting mechanisms.

1.1 Overview of the Existing Cell Sorting Mechanisms

Research regarding curing cancer diseases is one of the most challenging areas for researchers since the cell characteristics are difficult to manipulate in addition to their overlapping with the normal cells within the blood stream in the channels. Such challenges made it hard to find tools and approaches that lead to curing blood cancers and cancer tumors within the blood stream. The functioning and the production of the various types of blood cells were affected by the blood cancers, which alter the normal functioning of the blood. The cancerous tumor cells are produced in the bone marrow, and therefore, curing the disease is very challenging. Stem cells which are the basis of production for the various types of blood cells erythrocytes (red blood cells), leukocytes (white blood cells) and thrombocytes (platelets) [3], [4], [5]. The growth

factors of the healthy blood are interrupted by multiplication of the cancer cells. These malfunctioned cells degrade the normal functioning of the transport system, which transports nutrients, and oxygen to cells, impacting the immune system that fights against infection and clotting's, which prevent bleeding.

The current studies suggest that cell characteristics are highly heterogeneous in mammals in terms of size structure and genetic behaviors. For accurate analysis of a target cell which is under investigation [6], the cell sorting mechanisms are of significant value in cell studies and disease diagnosis [7], [8]. The existing conventional microfluidics methods re-viewed in [9], [10] for the cell sorting were based on affinity flow magnetic activated, cell separation, centrifugation, cyclometry, immunologic targets, chemotaxis phenomena, optical methods, light trapping, and electrophoresis, dielectrophoresis, and size based separation. These processes were done by pinched flow fractation [11].

1.1.1 Cell Sorting Based on Affinity

Affinity chromatography is used to separate the cells of interest from a mixture of cells using the affinity of the cells. This emphasizes the fact that this kind of separation is not a generalized one. This separation is done using the specific immunologic targets to capture or bind with a specific type of cells. This separation may be done using the positive selection where the immunologic targets bind with the desired cells of interest for separation or the negative selection where the bonded molecules are neglected and others were separated. Since the binding of the target cells needs high surface to volume ratio, microfluidic design for flow channels or reaction chambers play a major role in increasing the efficiency of the cell sorting.

Using the immunologic targets such as CD5 and CD19, Toner et al [12] have successfully separated the MOLT-3 cells from a mixture containing lymphocyte cell lines. Raji and MOLT-3 also, have reached similar outcomes under a sheer flow stress ranging between 0.75 and 1.0 dyn/cm^2. A two dimensional matrix device with circular

pillars is developed by the same group to increase the surface to volume ratio with a surface area of 970 mm^2 which successfully identified the cancer tumor cells from the blood with almost 99% efficiency [13]. The affinity and characteristics of HL60 and U937 using similar devices by Chang et al by a IgGchimera coated pillar than the existing non coated pillars [14]. This techniques have issues related to hindered or reduced flow rate and time consuming.

1.1.2   Cell Sorting Based on Size

Size based cell sorting in microfluidics has played important role in laying a path to research in the microfluidics Researchers have been working to investigate the size of cancer cells as compared to normal cells. As per the investigations, there is a general consensus that the cancer cells have bigger size than normal cells. This study was investigated in blood cancer, colon cancer, breast cancer. Several methodologies were been developed in the recent years to segregate the cells based on the sizes [15].

The applied magnetic force will not impact the structure of the normal cells however, since the cancer cells have the different structure, the force will impact them, and should be able to displace them based on their different sizes have quantified the cancer cell polarization properties with the magnetic field forces.

Microfilters

Initial development of microfluidic cell sorters is based on the microfluidic filters. The separation is done based on the pore size [16]. This technique failed due to clogging and limitations on number of cell types to be separated.

Separation Using Hydrodynamic Fluid Flow

The issues related to clogging and limitations on the number of cells etc., were enhanced by separating the cells based on the controlled flow rate and multiple outlets.

This design assumes the fact that the particle's center of gravity will flow along the stream line at low Reynolds number [17]. This technique faced issues related to the throughput, which needs an optimized channel structural dimensions, designed to construct an array of the similar structures with a single input.

The method has limitations when separating materials with specific change in their physical properties.

Separation Based on Deterministic Lateral Displacement(DLD)

This technique is an enhancement to overcome issues related to sorting range and clogging and the number of cells that can be sorted. This device contains a matrix of micro posts. This methodology is based on the fact that the interaction of cells with the micro posts in a laminar flow channel results in particle specific trajectories [18].

This technique have issues related to the critical size of the particles with there is no segregation occurs, and cells flow along with the streamline. This is further enhanced by changing the dimensions and gaps in the matrix of microposts [19].

Separation Based on Microfluidic Field Flow Fractionation

This technique is based on the fact that particles with higher surface area feels the high force profile. With this, cells are sorted based on their sizes in a microfluidic parabolic velocity flow profile device where the larger particles tends to move towards the wall and the other flow in the high velocity regions [20].

Separation Based on Microfluidic Micro structures and Hydrophoresis

This technique is based on the fact that the microposts, groves, herringbone structures play an important role in sorting mechanism. In this device the cells of different sizes and densities are driven to a specific stream using the protrusions [21].

Separation Based on Inertial Forces

This technique uses asymmetrical sheath flow and a novel structural design of the flow channel. The device is modeled to have a curved path to generate a inertial force that effects the fluid flow and the particle trajectories, based on their physical properties [22].

This techniques does not need any external fields or any sophisticated altering fluid flow. This device has issues related to clogging and limitations in sorting more than two types of cells.

Separation Based on Gravity and Sedimentation

This technique is based on the gravitational force on the microfluidic channel flow. The sedimentation of various particles depends on the radius, surface area of the particle interacting with another particle, viscosity and other fluidic properties. The separation distance between the two different particles is increased with the hydrodynamic effects towards the wide channel at the end of a curved channel design [23].

1.1.3 Cell Sorting Based on Intrinsic Characteristics

Separation Based on Biometric Separation

This technique is based on the bifurcation law which is called the Zweifach-Fung effect. This involves the hemodynamic flow characteristics pH of the blood in micro channels. This technique is used to separate the white blood cells [24], to separate cells from the blood plasma using the bifurcation law [25]. This has limitations in terms of sorting efficiency, and the multiple cell type sorting.

Separation Based on Magnetophoresis

This technique is developed by exploiting the fact that different type of cells have different intrinsic magnetic properties. This technique is used in separating the white blood cells from the red blood cells based on the fact that white blood cells are diamagnetic in nature while the red blood cells are paramagnetic in nature, and therefore, they move in opposite directions towards the channel wall away from channel flow [26].

This technique has a high potential since it explores the internal nature of the cells. Not many devices are developed based on this technique.

Separation Based on Aques Two Phase Systems

This sorting technique is developed based on the affinity of the cells towards a particular interface. A system is developed by SooHoo et al [27] using the PEG and dextran as two liquids and were able to segregate the white blood cells from the red blood cells. White blood cells did not enter the dextran phase while red blood cells were migrated to the other phase.

This technique has a huge potential since it explores the internal nature of the cells. Not many devices are developed based on this technique.

Separation Based on Acoustophoresis

This technique is unique compared to other sorting mechanisms where the sorting is done by acoustic radiation force when the channel is exposed to a ultrasound generator. Particles were sorted by forming a standing wave across the microfluidic channel. The cells are arranged towards the nodes and antinodes. Laurell et al has proved that the radiation can be altered for density based separation [28] and also size based on the sorting mechanisms [29].

Separation based on Dielectrophoresis

This technique is based on the principle that when a cell is placed in a non-uniform electric field, the exerted electric field creates a net force on the cell due to the induced or permanent dipole. The main potential of this technique is that the initial particle need not be a charged, and all the particles exhibit dielectrophoretic activity [30].

This is the reason it has been used for the development of various systems for selective trapping of particles, and modifying the flows.

1.1.4 Photocytometry Based Cell Sorting

The technique which uses light scattering to detect the various physicochemical characteristics of suspended cells is known as flow cytometry [31]. The initial step of flow cytometry is detection of individual cells by optical detection system which is achieved by hydrodynamic focusing. The flow rate is adjusted to thin stream in order to reduce cellular aggregation and clog the device micro fabricated channel structures, leading to accuracy, better flow and stable delivering samples The second step in this system is to sort out the cells at high speed, the redirection of flow via reverse electrokinetic and high speed valving, ultrasonic transducer, dielectrophoresis or optical trapping

1.1.5 Chemical Affinity Based Cell Sorters

In many physical and biological processes chemotaxis play a major role in healing, embryogenesis and in various cancer formation stages. It is a process in which a single cell, or multi cellular organism moves away or move towards a certain chemicals. It is estimated around 94% efficiency is achieved using this processes.

1.1.6   Need for a Design and its Solution

According to Grey N, et al., by 2030 there will be 23.6 million new cancer cases diagnosed, which is an alarming factor, almost 68% greater than the cases reported in 2012. This study emphasized the research in the development of early pre and post cancer detection devices.

Table 1.1.: Percentage of different types cancers.

#	Type of cancer	percentage
1	Lung Cancer	13.0
2	Breast Cancer	11.9
3	Bowel Cancer	9.7
4	Prostate Cancer	7.9
5	Stomach Cancer	6.8
6	Liver Cancer	5.6
7	Cervix Cancer	3.7
8	Oesophagus Cancer	3.2
9	Bladder Cancer	3.1
10	NHL Cancer	2.7
11	Leukemia	2.5
12	Pancreas Cancer	2.4
13	Kidney Cancer	2.4
14	Uterus Cancer	2.3
15	Lip Cancer	2.1
16	Thyroid Cancer	2.1
17	Ovary Cancer	1.7
18	Melanoma Cancer	1.6
19	Gall Bladder Cancer	1.3
20	Larynx Cancer	1.1

1.1.7   Importance of Cell Sorting Mechanism in Cancer Diagnosis

The main objective of the laboratory tests is to provide a detailed report of a individuals health condition by testing the samples of bodily fluids, tissues, cells, blood and urine. But in terms of the cancer diagnosis, separation of cancer blood cells or cancer tumors from the bulk plays a prominent role and enhances the identification of cancers by pathologists. This examination requires a lot of CLIA certified pathologists and highly sophisticated machines and environment. In addition to the laboratory tests, physicians use imaging tests to get more information about a patient condition.

This lab tests helps to screen precancerous and even the symptoms that leads to cancer, and stage of the cancer. But these tests are expensive and also require a large amount of time and effort. This motivates researchers to pursue more of the development of lab-on-chip devices that may give results in short time with minimum test costs.

Several microfluidic devices were developed using various concepts. But very few are have been commercialized. There is a need for a novel design which integrates various previously discussed design approaches to overcome all the limitations, and enhanced efficiency. There are no exact proof for data that is published with respect to the electrical properties of various types of cells. When compared with other researches there is a need for a device by integrating the concepts of sorting the cells based on both size and intrinsic properties, considering the practicality and efficiency.

Having defined a problem and proposed its solution, the presentation of this thesis details the issues, approaches, and results that prove the hypothesis of the research. A logical engineering approach includes the simulation reviewing the theory and defining the nature of the parameters to be investigated. Since in engineering terms, this involves the elements of dielectrophoresis, and integration of multiple concepts, the thesis details research concepts from both engineering and medical perspective.

1.1.8   The Thesis

While several cell sorting methods exist, there are barriers to their routine application for the cancer cell analysis, blood cell sorting. The existing methods to test cancer cells are expensive and time consuming. Since cancer is highly unpredicted there is a need for the development of cell sorting devices in order to increase the efficiency of rare cancer cell detection. There is a need to develop a multi cell sorting device to narrow the test sample quantity instead of bulk, reusable, low cost, efficient, and less time consuming. Such system could reduce the cost of the tests and reduce the diagnosis time to a large extent. A novel Approach for Cancer Tumor Segregation and Steering via variable field multi-microfluidic channels was achieved by exploiting the fact that cancer tumor cells and normal cells differ in size and charge. This was the basis of a novel multi level approach to segregate the normal cells from the CTCs (Cancer Tumor Cells) based on size, surface charges, resistivity, etc. Using dielectrophoretic and isoelectrophoretic forces, this device segregates the blood cells based on their sizes and surface charges. This device is a unit cell which can be further configured and multiplied based on the application.

2. PROPERTIES OF BLOOD PLASMA AND BLOOD CELLS

Blood is a consistently circulating fluid, providing the physique with oxygen required for cell functioning, nutrients to power the cells, and eliminates the waste products like carbon dioxide and other byproducts due to various biological reactions. Blood is an ordinarily liquid, with countless cells and proteins suspended in it, making it denser than pure water. The ordinary individual has about 5 liters of blood, of which near half from plasma that aides functioning the body system with proteins that helps with blood clotting, while the rest are from blood cells. Figure 2.1 gives the various forms of white and red cells within the blood. The average density of human blood is nearly $1060/Kg/m^3$. pH which is dependent on the partial pressures due to oxygen, carbon dioxide and carbonate ions in the blood is maintained between 7.35
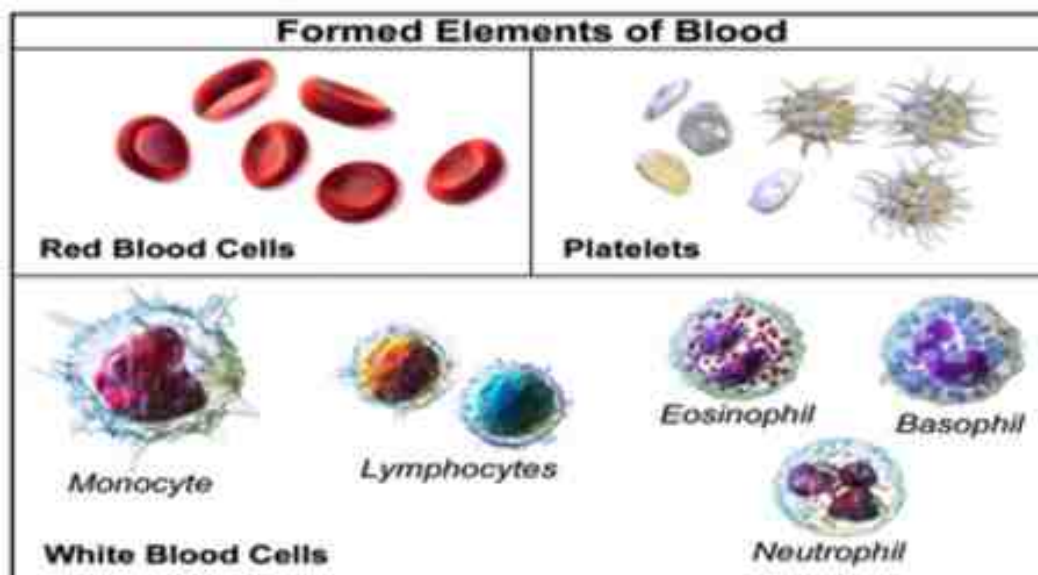
Fig. 2.1. Types of Blood cells.

to 7.45, a range that is required for the functioning stability. The flow of various cells and nutrients are required for the cell metabolism. The flow of the blood is through veins and arteries, which follows non-Newtonian fluid dynamics where the viscosity of the fluid is independent of time. The flow depends on the rate of normal and shears strain, and the amount of pressure on blood. Smooth and slipping blood vessel walls and continuous maintenance of clotting impact the viscosity and clotting of the blood. Table 2.1 depicts the cell counts within $1mm^3$.

Table 2.1.
Number of cells per mm^3 of blood.

Cell Type	Avg. Cell count	Min· Count	Max· Count
Erythrocytes	5400000	700000	6100000
leukocytes	7500	4000	11000
Thrombocytes	35000	20000	500000

The white blood cell (WBC) differentials with their numbers are given in table 2.2 [32]. The blood properties given in table 2.3 [33], may be utilized in the simulation model of the blood dynamics.

Table 2.2.
White blood cell differential.

Cell Type	Percentage	Min· Count	Max· Count
Neutrophil	50 60%	2000	6600
Eosinophils	1 4%	40	440
Basophils	0.5 2%	20	220
Lymphocytes	20 40%	800	4400
Monocytes	2 9%	80	990

Table 2.3.
Physical properties of blood at various frequencies.

Property	Units	100 KHz	1 MHz	100 MHz	100 GHz
Permittivity		5.12×10^3	3.03×10^3	7.68×10^1	8.30×10^0
Electrical Conductivity	S/m	7.03×10^{-1}	8.22×10^{-1}	1.23×10^0	6.34×10^1
Density	Kg/m^3	1050	1050	1050	1050
Thermal Conductivity	J/Kg/C	3617	3617	3617	3617
Heat transfer rate	ml/min/Kg	10000	10000	10000	10000
Heat Generation	W/Kg	0	0	0	0
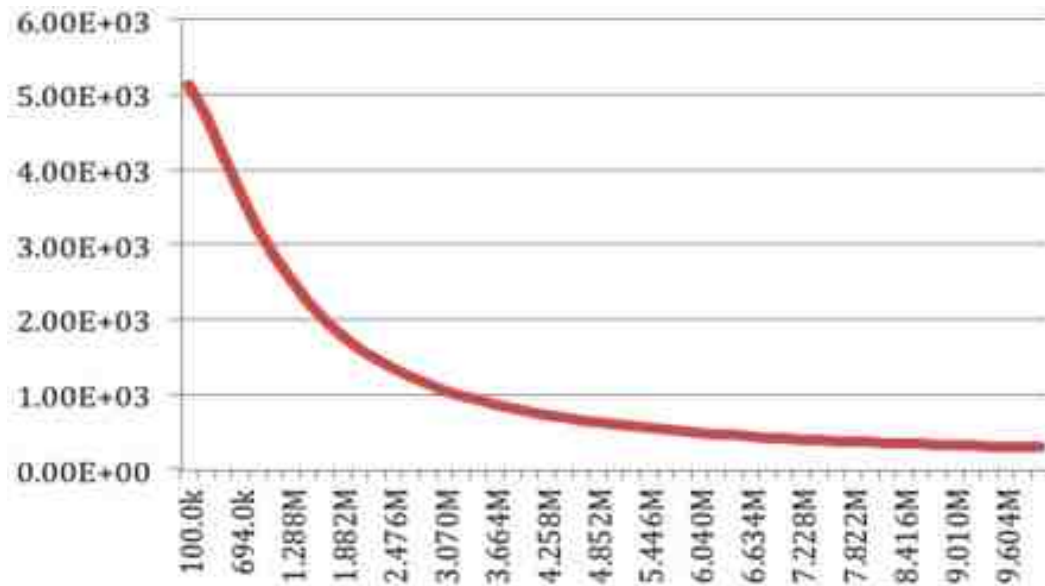
Fig. 2.2. Frequency Vs Permittivity of blood.

The dependency curve of permittivity and frequency is given in figures 2.2 and figure 2.3. As illustrated in the figures, the blood properties can be used for analysis of several diseases and state of blood.
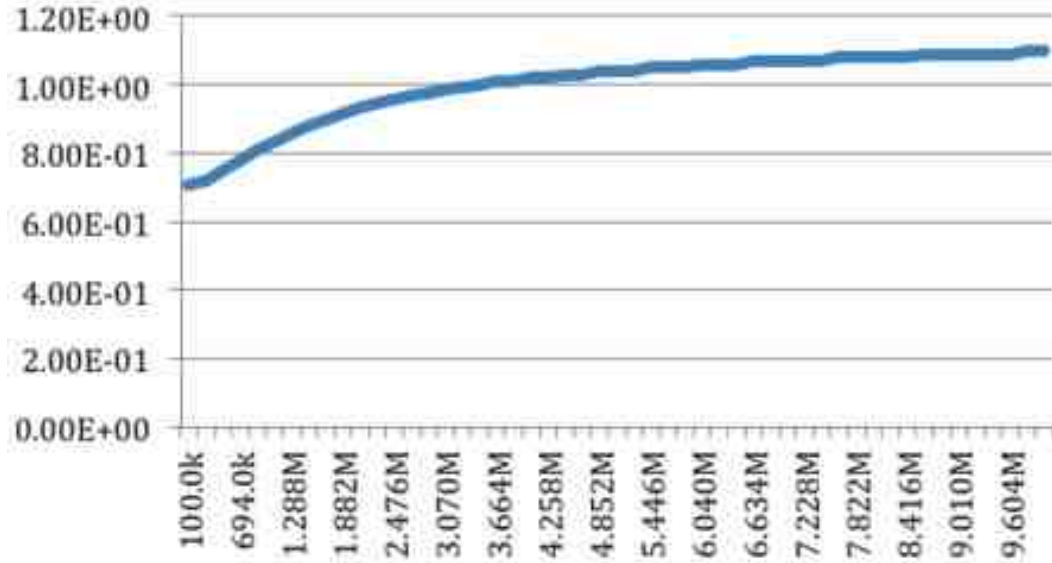
Fig. 2.3. Frequency Vs conductivity of blood.

Similarly, the electrical conductivity of the blood is also a function of frequency according to figure 2.3. At Lower frequencies up to 120 HZ, the average conductivity is near 6.50E-1 with a minimum of 0.6S/m and a maximum of 0.7S/m.

2.1 Cancer Cells Vs Normal Cells

The Study of the biochemical interaction is a paradigm to analyze the biological cell functions and their malfunctions over the past century, which leads to diseases in which some are curable, and still some of the diseases need a solution or a preventive medicines. But still there are several unanswered questions and enigmatic mechanisms that does not explain importance of electric currents or fields in the cell life process [34]. Since all the biological reactions output is in terms of electrons. There still however some standard study on the electric nature of the cells which may have the

potential to answer some of these important unanswered questions. Table 2.4 describes the differences between normal cells and cancer cells based on various characteristics of the cells.

Table 2.4.: Differences between cancer and normal cells.

Property	Normal Cell	Cancer cells
Structure of DNA	Regular DNA	Develops a modified DNA or Gene or alter the chromosomal count
Cell division	Controlled division	Uncontrolled cell division
Krebs Cycle	70%	0%
Glycolysis	20%	100%
Other	Aerobic 10%	Anaerobic requires Co_2
Cell transport system	They have a pre-built in blood vessels	They need to develop their own blood vessel systems using extra amino acids
Life cycle and growth factors	They grow normally and requires less supply of food	They grow abnormally and requires high food and functioning of the cells will be agile
Functioning	Balanced	Nonfunctional or over functional

The sensing and controlling activities of the human body is done by electric currents, the human body will have the ability to react to the EM fields [35], since the EM fields are related to the electrical current. From the table its clear that cancer affects the cell in almost all the regular characteristics of the cell. The study of the structural presented in the cells, which aid the data transmission and reception from other cells, emphasizes the sensing mechanism, memory storage, and the controller

that controls the cells and their processes. If someone says its DNA present in the nucleus that stores all the data and controls the cell, then arises a question why red blood cells function without the DNA. There is a need to study each and every difference in the characteristics of cell with respect to electrical properties and develop a mechanism for early detection of cancer instead of analyzing biochemical processes using antigens and antibodies. In this thesis, the future of cancer and other disease detection mechanisms based on the electrical properties, utilizing micro and nanofluidic bots at various parts of the body for regular monitoring will be investigated. One motivating fact regarding the cancer cells and the proliferating cells is that the potential of these cells were different from the healthy ones [36]. The cell communications network is disrupted due to the lower potentials of the cancerous tissues, causing the damage and growth of cancers to other parts of the tissue. In this thesis in order to obtain circuit model of cells, analysis for the restoration of healthy cell mechanisms were investigated. The steering electrode theory is based on device operation and manipulation to the cancer cells.

2.2   Cell Communication Networks

The functions of the cells are controlled by cell signaling receptors, which are mounted across the plasma membrane. This acts as port that receives the data from the cell signaling mechanism and transmits it to the nucleus. The port is connected to the core which is nucleus, and this is called the trans membrane receptor molecule. So when a signal is triggered in terms of a molecule or a protein or some sort of electrical impulse that leads to change in the shape or electrical characteristics, this will in turn generates a signal to the nucleus. The receiver proteins generate signals based on the signal received which turns on the DNA for the synthesis of proteins. Cancer is created when there is a disturbance in this part of the communication networks where the DNA is always turned on, leading to the continuous production of proteins, or to trigger the cell division. On the other hand, when the communication network
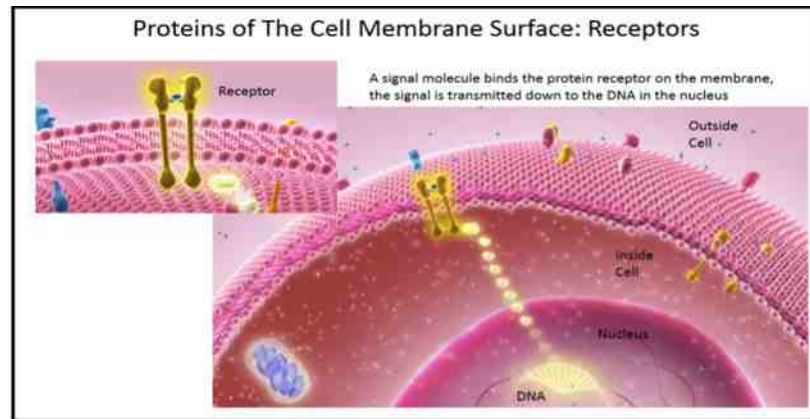
Fig. 2.4. Internal Cell Communication System.

is collapsed, it will lead to under functioning of cells leading to abnormalities in the cell structure. This cell signal transduction mechanism is clearly explained in the molecular communication networks section.

2.2.1 Molecular Communication Networks

In the diffusion based model, the propagation of molecules is due to the diffusion in the fluidic medium. In this process the molecular movement depends on the diffusion laws and sometimes turbulence in the fluid may also affect the communication. Calcium signaling between the cells is based on the molecular based communication through diffusion processes. A receiver model is designed based on the ligand receptor binding. An ideal model can be achieved through synchronization between the transmitter and receiving modules in a biological cell networks. [37].

Molecular motors/proteins are used to carry vesicles containing information in the form of molecular combinations is transmitted from the transmitter cell to the receiver. In order to enable reception, the transmitting module transmits protein tags that were tagged to specific receptors on targeted cell population.

Once the communication path is enabled between the transmitting and receiver cell, the communication process consist of following stages:

A) Encoding: This step involves the generation of the sensed data, which is to be transmitted and processed. This data is generated when an external stimulus to cell signal transmitter occurs. This processes involves the selection of appropriate molecules to depict the information or to invoke the reaction at receiver in this case nucleus of the cell. This enables us to control the reaction at the receiver for a particular stimulus applied to the transmitter.

B) Transmission: In this stage the encoded ligand molecules, which are proteins, are tagged to another larger molecule which are receptor molecules based on the affinity between them. If affinity between the protein molecules and receptor exists the information molecules bind with the molecular motors and transmission occurs. Alternatively, another biological methods like cell fission, pore formation or reproduction are used to transmit data packet in to transmission channel.

C) Propagation: This stages involves the transportation of information packets or molecules in the medium. Molecular rails or microtubules restrict the movement of these data packets. As a result, they align themselves with the rails instead of randomly moving or diffused in the medium similar to electrical signal propagation. The propagation speed depends on the information molecule and the molecular receptors and rails.

D) Reception: In this stage the molecular motors that tagged with information molecules are received by the receiving nano device where the information molecules are released from the molecular motors. A receiver may possess large number of reception properties in order to detach the data molecules from the carriers.

E) Decoding: The receiver core of the cell or other cells boosts the desired reaction based on the received data molecule. A biological cell consists of several receptors where each would be able to react with specific received molecule. Decoding is a sensitive process and dependent on the specific receptors. Alternatively, information can be decoded within a cell where the cell having single receptor and the different data uses same interface like vesicles.

Any errors in the above stages may lead to corrupted data or complete loss of data which may trigger wrong functions or degrade the functioning of the cells. Thus it opens a new area of research to repair the cells through cell signalling.

2.3 Cancer Cells Vs Temperature

The temperature of the cancer cells is high when compared to normal cells. This is due to the continuous replication process, exo and endothermic energy producing mechanisms. The increase in glycolytic flux also leads to increase in cell temperature.

2.4 Electrical and Magnetic Properties of Normal Cells and Cancer Cells

Early in 70s it was proved that the DNA of the cell is not the cause of the cancer. This was proved by replicating the nucleus of mouse fertilized egg by a cancerous nucleus which resulted in a cancer free mice [38]. This has triggered the study on other parts of the cells, including the cancerous nature in cells. The defects in cell membrane and the disturbance in the mitochondrial energy production mechanism caused the cancer which are supported by testing a cell by deactivating enzymes supply to the mitochondria resulted in cancerous cell [39]. It was also found out that cancerous nature in cells results in high electronegative behavior when compared to the healthy cells.

From the above studies it was clear that more research is needed in order to validate the controlling of the carcinogenic agents in the blood that effect the mitochondrial functioning continuous monitoring of carbon dioxide levels in blood, tissue, blood vessels through micro or nano bots, helps early detection mechanisms. Developing micro devices is important in order to continuously monitor the blood vessels to find the carcinogenic elements and deactivate them continuously. This chapter describes the various electrical, magnetic, and metabolic properties of normal and abnormal blood cells.

2.5 Biological Cell in Terms of Charge Regions.
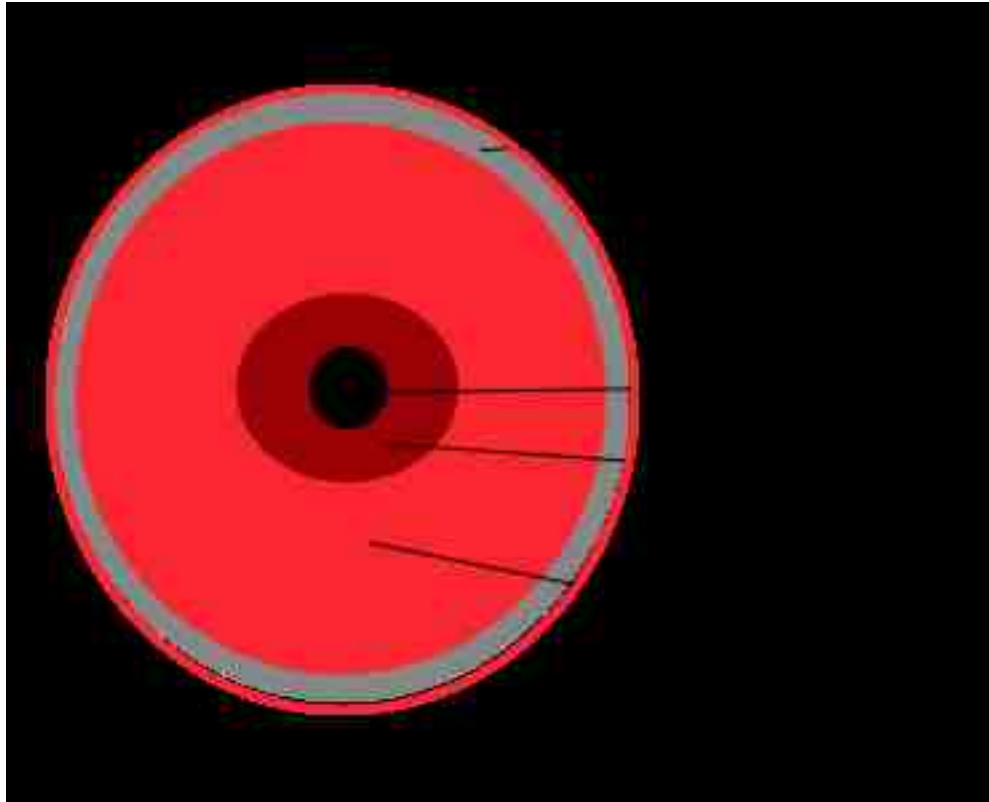
Fig. 2.5. Electric Insulation.

2.6 Comparison of Cell Structures to the Electrical Components

Capacitors hinders the flow of current by storing it in the form of electric fields. This triggers the fact that the electric fields play a major role in both AC and DC electric mechanisms or systems. When the biological mechanisms are signaled, and their functions are based on the pulsating DC [40] and AC [41] currents. This triggers the development of analyzing mechanisms based on the charges, and this is an intrinsic characteristic of various different cells and tissues and the alternating field effects were .

2.6.1 Capacitive Effect of Plasma Membrane

The alternating effect in this case where capacitive because the membrane plasma is proportional to both the size, surface area and charge across the membrane. This leads to segregation of cells based on their sizes and charges.

Separation Based on Charges

The plasma membrane of the cells is defined as a poor dielectric and its parameters vary based on the health of the cell and environment of the cell. This supports the fact that when the capacitance is altered, the charge will be also proportionally altered allowing healthy and cancerous/malignant cells to be separated based on their charges.

Separation Based on Sizes

Since the capacitance is directly proportional to the area, which in turn proportional to total charge, larger cells have higher charge.

2.7 Surface Potential of Cells

The cell membrane which is also called the plasma membrane functions as a battery where the trans membrane or the crystalline aqueous cytoskeletal proteins are developed to power the cell structures like the nucleus, DNA etc., Studies suggests that very high electric fields were required for interacting with the cells. The potential across the plasma membrane is between 10,000,000V/m [42] and 20,000,00 V/m [43]. Taking the average of the two studies it is about 15,000,000V/m which is relatively very high potential.

This studies trigger the fact that very high electric fields were required for interacting with the cells. The mitochondrial potential formed due to positive hydrogen ions is about 40,000,000 V/m. So any electrical mechanism that needs to interact

with mitochondria should be able to deal with such high surface potentials. Table 2.5
gives the information and comparison between healthy and cancer cells describing the
chemistry that triggers the electrical properties.

Table 2.5.
Comparison of healthy cells with cancer cells.

Property	Normal cells	Cancer cells
Membrane potential	-60 to -100	Less than healthy cells based on their type
Potential at Inner surface	Negative relative to external surface	-
Trans membrane potential	10,000,000 to 20,000,00	Less
Concentration of Potassium	High	Potassium, Magnesium and Calcium and zinc are lost
Concentration of Sodium	Low	Water and Sodium leaks in from surface membrane
Electronegativity	Low	High

2.8 Cell Characteristics Influencing Zeta Potential

The sialic acid, with negative charge residues determine the zeta potential of a
cell over the plasma membrane. Since the amount of sialic acid determines the pH of
the cell and zeta potential any factors that influences the concentration of cells leads
to alteration in the zeta potential. This triggers the use of uniform electric fields for
the development of separation mechanisms. Cancer cells will have lower pH due to
agile glycolytic activity leading to producing the acid equivalent in a abnormal cell.

2.9   Magnetic Properties of Blood Cells

Since the blood consists of hemoglobin which is a rich constituent of Fe(Iron) leading to the paramagnetic nature of the deoxygenated erythrocytes which contain hemoglobin [44]. To overcome the issue of maintenance the paramagnetic behavior of erythrocytes, cells were treated with $NaNO_2$ which reacts with hemoglobin and produces meta-hemoglobin which is paramagnetic.

With the help of Biot-Savart law [45] the concentration of field at a point which is at a distance of r from the center of the cell is given by,

$$\triangle B(r) = \frac{\chi}{4\pi} \int \frac{B_0 \times n \times (r - R)}{\|r - R\|^3} dS(R) \tag{2.1}$$

where χ is the intercellular susceptibility, and n is normal unit vector to the surface at a point R. The cross product between B and n is dependent on the cell orientation. The white blood cells are diamagnetic and are repelled away from the high fields.

Using this difference in magnetic behavior of red blood cells and other cells. This was the model concept of the device to separate RBC's in their initial stages using magnetophoresis.

3. DIELECTROPHORETIC SEPARATION OF CELLS

Particles in a non-uniform electric field develop an induced dipole and spatial gradient of the applied electric fields which results in deviation of particles from normal movement. The total force exerted on a particle is obtained when a electric field is applied in both time and frequency domains. The following characterizes the particles with in the frequency domain,

$$F_{ext} = 2\pi(r)^3 real(\varepsilon_f^*) real\left(\frac{\varepsilon_p^* - \varepsilon_f^*}{\varepsilon_p^* + 2\varepsilon_f^*}\right)\nabla\|E_r ms\|^2 \tag{3.1}$$

where ε_f^* ε_p^* are the complex relative permittivity of the fluid and particle. The root mean square of the electric field is given by E_{rms}.

The complex permittivity calculated in the frequency domain is given by the following relation,

$$\varepsilon^* = \epsilon - \frac{i\sigma}{\omega} \tag{3.2}$$

where ϵ is the permittivity, electrical conductivity σ, angular frequency of the applied electric field ω of the fluid or particle.

Since the cells possess a thin shell, which is called the cell membrane or the cytoplasmic membrane, we need to consider the shell parameters of the cells. Since the shells play the major role in defining the healthy and abnormal cells we need to consider the shell permittivity in order to study the electric force on the cell. The complex permittivity of the cell can differ from the cytoplasmic or the shell permittivity. The permittivity of the cell is replaced by the homogeneous complex permittivity by calculating equivalent permittivity from the following relation.

$$\varepsilon_{eq}^* = \varepsilon_s^* \frac{\left(\frac{r_0}{r_i}\right)^3 + 2\left(\frac{\varepsilon_p^* - \varepsilon_s^*}{\varepsilon_p^* + 2\varepsilon_s^*}\right)}{\left(\frac{r_0}{r_i}\right)^3 - \left(\frac{\varepsilon_p^* - \varepsilon_s^*}{\varepsilon_p^* + 2\varepsilon_s^*}\right)} \tag{3.3}$$

where r_0 and r_i are the inner and outer radius of the shells, and the ε_s and ε_p are the complex relative permittivity's of the shell (cytoplasmic membrane) and the other parts of the cell.

3.1 Particles with Attenuated Cell Membranes

Since some of the cells are very thin in the nanometer range cytoplasm which is either conductive or resistive plays a major role in studying the dielectric behavior of the cells and their interactions with electric fields. Considering the fact that the shell thickness δ and R_0 is outer radius of the shell and R_i is the inner radius of the shell,

$$R_0 = R_i + \delta \tag{3.4}$$

$$where \delta << R_i \tag{3.5}$$

Surface capacitance plays a major role when the charge flows across the cell membrane becomes dominant. The surface capacitance can be defined as:

$$c_m = \frac{\varepsilon_s}{\delta} \tag{3.6}$$

and the transmembrane conductance is given by g_m

$$g_m = \frac{\sigma_s}{\delta} \tag{3.7}$$

assuming the fact that $\frac{\delta}{R} << 1$ where $R \equiv R_i$ and substituting the equations 3.7, 3.8 in equation 3.5 reduces the equation to:

$$\varepsilon_{eq}^* = \frac{c_m^1 R \varepsilon_p^1}{c_m^1 R + \varepsilon_p^1} \tag{3.8}$$

where:

$$c_m^1 = c_m + \frac{g_m}{j\omega} \tag{3.9}$$

There may be a case where the ion transport in the cell is tangential to the surface of the particles, then the dielectric constants were altered. This altered dielectric constant $\varepsilon_e q$ is given by the following relation:

$$\varepsilon_e q = \varepsilon_p^1 + 2\frac{\varepsilon_\Sigma^1}{R} \tag{3.10}$$

where:

$$\varepsilon_\Sigma^1 = \varepsilon_\Sigma + \frac{\sigma_\Sigma}{j\omega} \tag{3.11}$$

and:

$$\sigma_\Sigma = \delta\sigma_s \tag{3.12}$$

$$content... \tag{3.13}$$

The figure below depicts the interpretation for the equations 3.9 to 3.13 with equivalent electric circuit. The cytoplasm membrane of a biological cell consists of some cell proteins which acts as a dielectric material which alters the cell electrical properties. Equation 3.11 deals with the parallel conductance due to the tangential permittivity ε_Σ leading to produce induced out of phase motion of cytoplasmic ions tangential to the membrane and influences cell cytoplasmic conductance σ_Σ. Since the membrane is thin and some cells cannot be polarized and they can be ignored by removing the $\varepsilon_\Sigma << \sigma_\Sigma/\omega$ term leads to:

$$\varepsilon_{eq} = \varepsilon_p^1 + \frac{\sigma_{eff}}{j\omega} \tag{3.14}$$

where the ohmic conductivity of the equivalent particle is given by:

$$\sigma_{eff} \equiv \sigma_p + \frac{2\sigma_\Sigma}{R} \tag{3.15}$$

3.2 Orientation of Irregular Shape Particles to the Field

Irregular and non-spherical shaped cells are more common in biological cell types than the spherical particles. Red blood cells which are more in number are oval shaped. This leads to analyzing the particles based on three axis of orientation with three semi-major axes. For a red blood cell the three axis are in 4:2:1 ratio. This irregular shape adds geometric anisotropy to a cell, if the cell is aligned to one of the

axis parallel to the applied electric field then it results in induced dipole moment to the particle. The average moment of the non-spherical cell with semi -major axis x, y, z is written as:

$$P_{eff}^- = \frac{4\pi xyz}{3}(\varepsilon_s - \varepsilon_f)\bar{E}^- \tag{3.16}$$

where E^- is the intrinsic electrical field that is localized to the cell, which is not **always** parallel to $\overline{E_0^-}$.

$$E_x^- = \frac{E_{0,x}}{1 + \frac{(\varepsilon_s - \varepsilon_f)L_x}{\varepsilon_f}} \tag{3.17}$$

Where:

$$L_x \equiv \frac{xyz}{2}\int_0^\infty \frac{ds}{(s+x^2)R_s} \tag{3.18}$$

Where:

$$R_s \equiv \sqrt{(s+x^2)(s+y^2)(s+z^2)} \tag{3.19}$$

Similarly the y component of the intrinsic electric field is given by:

$$E_y^- = \frac{E_{0,y}}{1 + \frac{(\varepsilon_s - \varepsilon_f)L_y}{\varepsilon_f}} \tag{3.20}$$

Where:

$$L_y \equiv \frac{xyz}{2}\int_0^\infty \frac{ds}{(s+y^2)R_s} \tag{3.21}$$

Similarly the azimuthal component (z) of the intrinsic electric field is given by:

$$E_z^- = \frac{E_{0,z}}{1 + \frac{(\varepsilon_s - \varepsilon_f)L_y}{\varepsilon_f}} \tag{3.22}$$

Where:

$$L_z \equiv \frac{xyz}{2}\int_0^\infty \frac{ds}{(s+z^2)R_s} \tag{3.23}$$

The total dielectrophoretic force and torque on a non-spherical cell is given by substituting equation 3.17 in the torque approximation, yielding to:

$$\bar{T} \approx \bar{p} \times \bar{E}_0 \tag{3.24}$$

Where the effective moment $\bar{P}_{eff}$ is defined as:

$$P_{eff}^{-} \equiv 4\pi\varepsilon_f K R^3 \bar{E}_0 \qquad (3.25)$$

K is the Clausius-Mossotti factor. The x component of the resultant torque is given by:

$$T_x^e = \frac{4\pi xyx(\varepsilon_s - \varepsilon_f)^2(L_z - L_y)E_{0,y}E_{0,z}}{3\varepsilon_f\left[1 + \left(\frac{\varepsilon_s - \varepsilon_f}{\varepsilon_f}\right)L_y\right]\left[1 + \left(\frac{\varepsilon_s - \varepsilon_f}{\varepsilon_f}\right)L_z\right]} \qquad (3.26)$$

The y component of the resultant torque is given by:

$$T_y^e = \frac{4\pi xyx(\varepsilon_s - \varepsilon_f)^2(L_x - L_z)E_{0,z}E_{0,x}}{3\varepsilon_f\left[1 + \left(\frac{\varepsilon_s - \varepsilon_f}{\varepsilon_f}\right)L_z\right]\left[1 + \left(\frac{\varepsilon_s - \varepsilon_f}{\varepsilon_f}\right)L_x\right]} \qquad (3.27)$$

The z component of the resultant torque is given by:

$$T_z^e = \frac{4\pi xyx(\varepsilon_s - \varepsilon_f)^2(L_y - L_x)E_{0,x}E_{0,y}}{3\varepsilon_f\left[1 + \left(\frac{\varepsilon_s - \varepsilon_f}{\varepsilon_f}\right)L_x\right]\left[1 + \left(\frac{\varepsilon_s - \varepsilon_f}{\varepsilon_f}\right)L_y\right]} \qquad (3.28)$$

Assuming positive three dimensional electric field and the semi-axis ratio $x > y > z$, the relation, $0 < L_x < L_y < L_z < 1$, can be written. This results in $T_x^e > 0 T_y^e < 0 T_z^e > 0$, which clearly depicts the resultant torque due to electric field will be along one axis, and this should be the longest and parallel to the applied field. The resulting torque will be stable and does not rotate. The characteristic moments in prolate and oblate cell structures are considered as a special cases. Since the cells are flexible and tends to deform due to cell interactions and external forces, this may result in aligning them with the applied electric field. The three axes become dominant, depending upon the relative permittivity and conductivity of the cell at specific frequency ranges. The alignment and moment of the non spherical cell lies in selecting the low and high frequency boundaries is the major axis. If the cell is aligned with the shortest axis then the cell will flip based on the threshold frequencies. These threshold frequencies that alters the moment of particles are called the orientation frequencies [15]. These turnover frequencies are due to the Maxwell-Wangner charge relaxation time for each unique three dimensional orientation. The resultant torque mentioned in the above

equations can be used to determine the ellipsoids and spherical cells, considering that the torque and the complex permittivity are different for each axis. The blood cells are flexible and alter their shape in case of collisions and high electromagnetic fields. Study of orientation of irregular shapes pays a major role in enhancing cell sorting.

3.3   Dielectrophoretic Trap

The cells can be trapped or captured or sorted form other cells suspended in the microfluidic channel. The cells can be trapped or collected if the induced force is greater than the drag force.

The Mathematical model that control the particle operation is described as:

$$\|F_{dep}\| > \|F_{drag}\| \tag{3.29}$$

From stokes law:

$$F_{drag} = 6\pi\eta r_p v(x) \tag{3.30}$$

Where r_p is the radius of the cell, $v(x)$ velocity of the fluid in the channel.

For a rectangular microfluidic channel with parabolic fluid flow the velocity of the dielectric particle of radius r_p and at a position d_p is given by:

$$v = v_x(d_p)\hat{e}_x \tag{3.31}$$

This can be written from the parabolic flow equation as:

$$v_p = 6\left[1 - \frac{d_p}{W}\right]\frac{d_p}{W}v_f\hat{e}_x \tag{3.32}$$

Where v_f is velocity of the fluid and v_p is the velocity of the particle. d_p is the distance of the particle from the ground wall, and W is the width of the microfluidic channel.

We know that the force due to the dielectrophoresis on a dielectric cell or particle is given by:

$$F_{dep} = [P.\nabla]E \tag{3.33}$$

The induced polarization on a cell or particle of radius r_p and dielectric constant ϵ_p due to dielectrophoresis is obtained by Substituting the F_{dep} in equation 3.33:

$$P = 4\pi\varepsilon_p \frac{\varepsilon_p - \varepsilon_f}{\varepsilon_p + 2\varepsilon_f} r_p^3 E_\Phi \tag{3.34}$$

Particle Trapping will take place close to the electrode but in our system the particles are pulled towards the electrode and exited out through a outlet. Assuming that the outlet channel is close to the electrode and the particles will flow through the outlet whenever it come near to the electrode with radius $r_e << W$.

Form the above relations the dielectrophoretic force at the electrode is given by:

$$F_{dep}(r_e) = [P(r_e)\nabla]\, E_0(r_0) \tag{3.35}$$

substituting equation 3.34 in 3.35 gives:

$$F_{dep}(r_e) = 4\pi\varepsilon_p \frac{\varepsilon_p - \varepsilon_f}{\varepsilon_p + 2\varepsilon_f} r_p^3 [E_0(r_e).\nabla] E_0(r_e) \tag{3.36}$$

Equation 3.36 can be rewritten as based on the following identity:

$$2E \cdot \nabla E = \nabla[E^2] \tag{3.37}$$

substituting equation 3.37 in 3.36 gives the dielectrophoretic force near the electrode gives:

$$F_{dep}(r_e) = 2\pi\varepsilon_p \frac{\varepsilon_p - \varepsilon_f}{\varepsilon_p + 2\varepsilon_f} r_p^3 [E_0(r_e)^2] \tag{3.38}$$

The electric field E at a distance r form the electrode is given by:

$$.E(r) = -\nabla\Phi(r) \tag{3.39}$$

$$\approx \frac{r_e \Delta V}{r} \hat{e}_x \tag{3.40}$$

Where $r_0 < |r| << W$ and substituting equation 3.40 in 3.38 gives:

$$F_{dep}(r_e) = 2\pi\varepsilon_p \frac{\varepsilon_p - \varepsilon_f}{\varepsilon_p + 2\varepsilon_f} r_p^3 \nabla \left[\frac{r_e^2 \Delta V^2}{r^4} r_e^2 \right] \tag{3.41}$$

Differentiating the above equation with respect to the electric field gives:

$$F_{dep}(r_e) = 8\pi\varepsilon_p \frac{\varepsilon_p - \varepsilon_f}{\varepsilon_p + 2\varepsilon_f} r_p^3 \frac{r_e^2}{r^5} (\Delta V)^2 \hat{e}_r \tag{3.42}$$

F_dep is maximum when the particle is near to the electrode. The proposed system exits the cell through an outlet so that cell may get trapped i.e., when the cell comes near to the electrode and the outlet vicinity, the distance from the electrode will be minimum, and the force acting on the cells will take the resultant value to stay near the electrodes until the exit:

$$r_{min} = r_e + r_t \tag{3.43}$$

where:

$$r_t = (r_{out} - r_p) \tag{3.44}$$

Assume a constant β such that $\beta = \frac{r_e}{r_t}$ equation 3.42 reduces to:

$$F_{dep}(r_e) = 4\pi\varepsilon_p \frac{\varepsilon_p - \varepsilon_f}{\varepsilon_p + 2\varepsilon_f} \frac{\beta^2}{(1+\beta)^5}(\Delta V)^2 \tag{3.45}$$

Substituting r_t in equation 3.32 gives:

$$v_t = 6\left[1 - \frac{(1+\beta)}{r_t}W\right]\frac{(1+\beta)}{r_t}WV_0 \tag{3.46}$$

$$v_t \approx 6(1+\beta)\frac{r_t}{W}V_0 \tag{3.47}$$

Substituting equation 3.46 in Naiver stokes equation 3.30 gives F_drag at a distance r_t:

$$F_{drag}(r_e + r_t) = 6\pi\eta r_p v(r_e + r_t) \tag{3.48}$$

$$F_{drag}(r_e + r_t) \approx 36\pi(1+\beta)\eta\frac{r_t^2}{W}V_0 \tag{3.49}$$

Equating 3.48 and 3.42 gives the maximum velocity of the fluid at a voltage v leads to trap the cells or particles through the outlet is given as:

$$v_0^{max} = \frac{2}{9}\frac{\varepsilon_p - \varepsilon_f}{\varepsilon_p + 2\varepsilon_f}\frac{\beta^2}{(1+\beta)6}\frac{W\varepsilon_f(\Delta V^2)}{\eta r_t^2} \tag{3.50}$$

3.4 Simulation Assumptions and Approach

The simulation model is based on ideal conditions. The wall of the microfluidic channels were considered to be bouncing and the backflow of the fluid is suppressed. The cell parameters were given assuming the cell as a spherical shell. The parameters for the outer surface and inner cells surface were defined relatively with respect to the normal cells. Based on the fact that the cancer cells and malfunctioning cells in the blood stream has a lower potential, higher conductivity, thinner cell membranes, the model is tested for various sizes and shapes. The numerical models for the voltage supply is derived by extending the trapping distance of the cell by an exiting channel width. The electric field produced by a semicircular electrodes is higher than the rectangular electrodes, leading to achieving high energy with a lower electrode voltage ,an reasonable assumption that preserve the cancer cells from dying. This result may contribute to the MRD (Minimal Residual Disease) application, where smaller voltage can achieve the desired path of the particles.

4. COMPUTER AIDED DESIGN AND COMSOL SIMULATION

The Device modeling is done using the COMSOL multiphysics software which is a very appropriate platform for Physics-based modelling and simulation. This software helps in studying coupled and integrating multiphysics phenomena. The multiphysics simulations can be integrated with external software's such as MATLAB and CAD. This software also helps with incorporating the device physics and the mathematical models of the system. The multiple add-on products provided by COMSOL assisted in interfacing the different modules of the integrated system.

4.1 Modules used for Device modeling

The proposed device needs to integrate the electrical performance, magnetic eld performance, and particle interactions. Fluid flow in micro channels, particle tracing physics, and visual graphics are all integrated into one system. This was accomplished by integrating the AC/DC module, microfluidics module, and particle tracing module for achieving accurate simulation results.

4.1.1 AC/DC Module

This module is used for simulating the electromagnetic fields at low frequencies. The electrical and magnetic properties of designed models were also simulated for the purpose of studying the capacitance, force, resistance, torque, conductance, and impedance. When dealing with the complex circuits this module can be interfaced with the SPICE software through ECAD import modules. The proposed model requires the boundary conditions for simulating the electric and magnetic fields, and

terminal conditions for floating potentials. Symmetric conditions regarding surface currents and impedances, distributed capacitance, impedance and contact resistance were incorporated. Infinite elements were also available for electric and magnetic field study.

Since the device modeling is based on the study of thin shells and micro sized particles, this module fits well since it provides a varied range of sophisticated equations for efficient EM simulations.

Electric Currents Interface

Electric current Interface is used to analyze the electric field and potential distributions in a conducting medium where effects due to induction are minimum. This interface is important in conserving the formulation based on the Ohms law. The field equations emphasize the scalar and vector potentials.

Conservation of the current is the main node in the interface, which solves for the electric potential. The parameters for the electrical conductivity, equations for the electric displacement field, material properties of the medium can be modified based on our design.

4.1.2   Microfluidics Module

Since the proposed device is at micro scale, so studying the hydrodynamic effects on cells would be the key in the device simulation. This module helps in modeling and achieving accurate results virtually. The net fluid flow is achieved by a electric field which moves the unbalanced ion concentration that is present in the charged EDL (Electric double layer) on the fluid surfaces. This process is called electroosmosis. A sophisticated boundary conditions for the electroosmotic velocity can be defined using the microfluidics module along with other boundary conditions. Electrophoretic and dielectrophoretic forces on charged or polarized particles in the fluid can be used to induce particle motion, and diamagnetic forces in the case of magnetophoresis.

Creeping Flow Interface

Creeping flow interface is used to study the single phase flow at very low Reynolds number. The inertial term in the Navier-Stokes fluid flow equation is discarded due to low Reynolds number. This flow is also referred to as a Stokes flow, which is common in microfluidic devices.

Conservation of momentum and continuity equations are solved by the creeping flow interface in the microfluidics module.

4.1.3 Particle Tracing Module

The trajectory of the cells in the fluidic medium in the presence of the electromagnetic fields can be computed using the particle tracing module present in the COMSOL multiphysics software. Various types of interactions between cell-cell, cell-wall, fluid-cell, wall-cells are computed for a complete near real-time simulation results. This module can be extended to compute the fields that contribute to the particles or cells motion. The defined particles may have defined mass or some may be massless. The trajectory of the particles are computed by using the Newtonian, lagrangian, Hamiltonian governing equations that are defined in classical mechanics. The boundary conditions can be defined for the call-wall interaction. This conditions can be defined for various cases like freezing the cell, stick to the wall after touching the wall, bouncing walls, disappear after touching the wall, cells can be defined to reflect diffusively after interacting with the wall of the channel. This module provides the feasibility of user defined wall conditions. This user defined conditions are used for the chemical reactions, energy absorption, excitations phenomena, or when the velocity after collision is a function of the interacting particle or cell. The number of particles, time dependent particle release or a particle number and release times can be defined using a user defined function. A new particles can be defined to be released after primary particle interacts with the wall. The secondary cell or particle's velocity function, number can also be defined as a function. Particles can also stick

to the channel boundaries based on user defined functions or based on probability functions. Particles mass, temperature, orientation of the particle (spin) can also be calculated by using the additional dependent variables.

Particle interaction with the fields can be defined using various forces thet are predefined in the module. User defined arbitrary forces can also be simulated using this module.

The Particle Tracing Module provides ready-to-use electrophoretic and dielectrophoretic particle forces. Combining the Microfluidics Module with the AC/DC Module enables to model AC dielectrophoresis.

4.2   Device Modeling

The device is modeled based on the COMSOL Multiphysics model Dielectrophoretic separation of platelets from red blood cells. This model demonstrates the continuous separation of the red blood cells from platelets using the dielectrophoresis.

The modeling and enhancement of the cell sorting device is divided into eight phases. The modeling of the device starts with the selection of model wizard.

This section describes every phase in the design.

4.2.1   Phase 1: Model Wizard

The proposed device is modeled initially in 2- dimensional space, neglecting the z-axis. Then the required physics modules for simulating the device are selected. In this case we choose the Electric Currents (ec) interface from the AC/DC module to study the fields. Creeping Flow (spf) interface is selected from the microfluidics module. Particle tracing for fluid flow (fpt) is selected from the particle tracing module.

4.2.2 Phase 2: Geometry and Device Design

Device structure is modeled in this phase. Figure 4.1 depicts the construction of the simple unit cell sorting model.
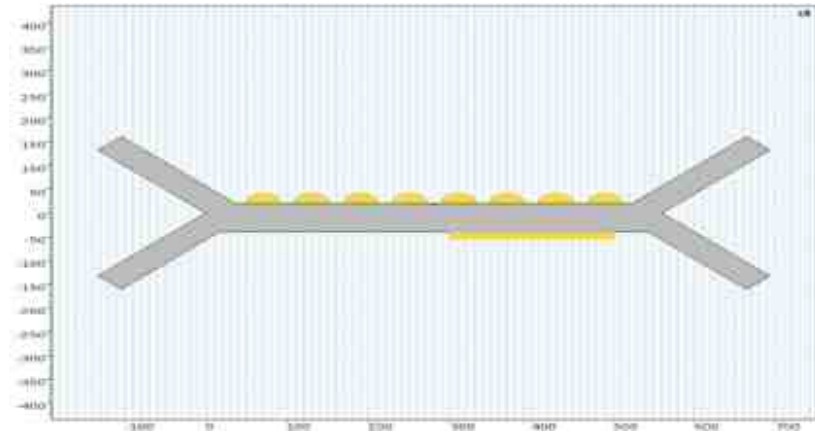
Fig. 4.1. Structure of Unit cell sorter.

This is further expanded and used to construct the various models for designing the efficient cell sorting layout. Figures 4.2, 4.3 and 4.4 depict the various models that were developed using the unit cell.
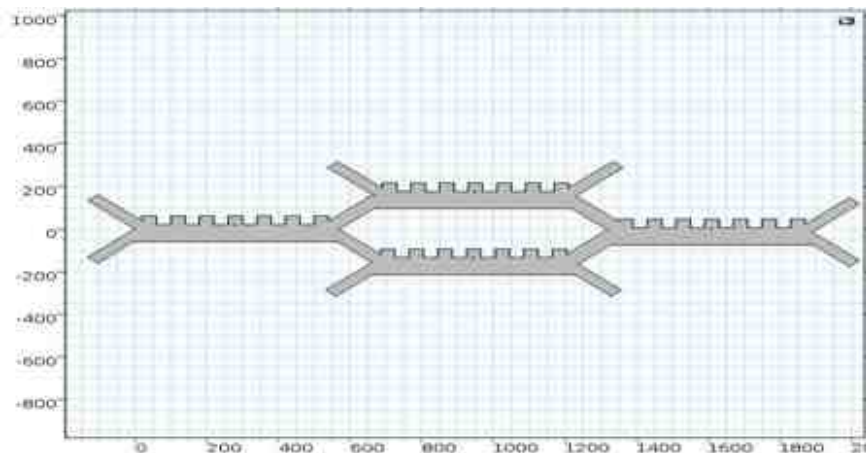
Fig. 4.2. Quadruple cell sorter Linear model.
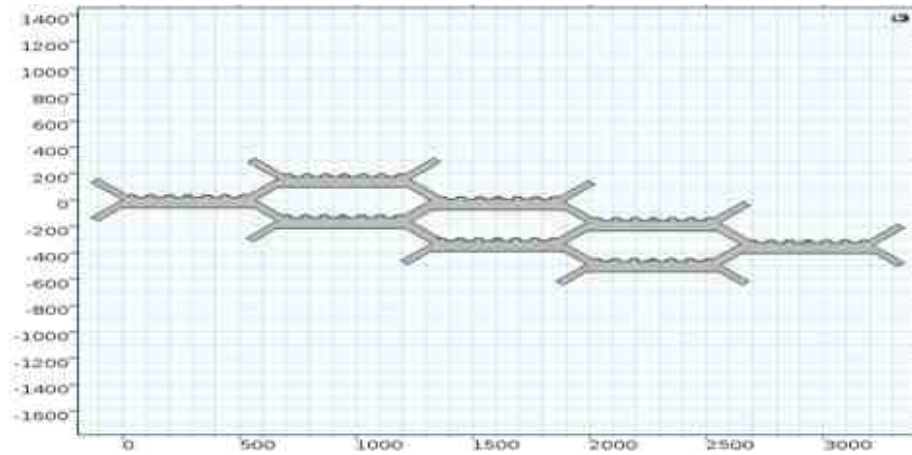
Fig. 4.3. Six cell sorter Linear model.
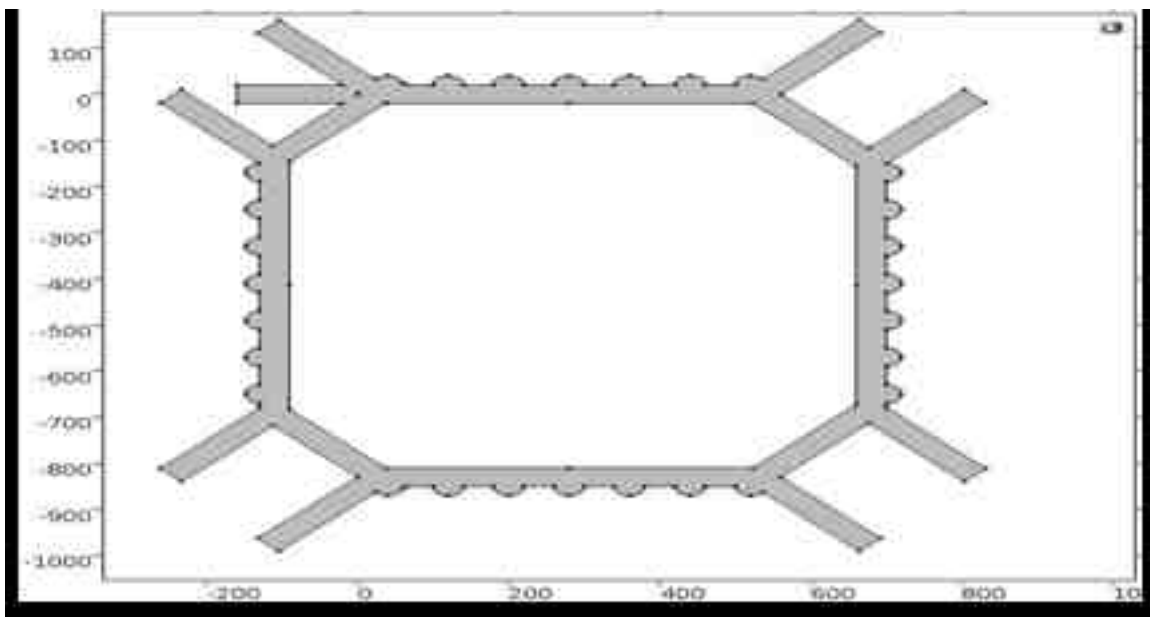
Fig. 4.4. Quadruple cell sorter.

In this model the Electrodes are converted to solid which is an enhancement from the existing model that uses a surface electrode. The advantages of using the semicircular electrode are discussed in the results section.

4.2.3   Phase 3: Definitions

In this phase, the parameters for the device, fluid, electric field frequency defined are defined. These parameters are used in the modeling of the integrated system. Table 4.1 represents the parameters given for the initial simulation of the multi cell sorter.

Table 4.1.: Parameters used for the design.

Property	Description	Value
f0	$100[kHz]$	Frequency of the electric field
sigma_f	$55[mS/m]$	Fluid medium conductivity
epsilon_f	80	Fluid relative permittivity
rho_f	$1000[kg/m^3]$	Fluid density
mu_f	$1e-3[Pa*s]$	Fluid dynamic viscosity
rho_p	$1050[kg/m^3]$	Particle density (RBCs and platelets)
dp1	$1.8[um]$	Particle diameter: platelets
dp2	$5[um]$	Particle diameter: RBCs
sigma_p1	$0.25[S/m]$	Particle conductivity: platelets
sigma_p2	$0.31[S/m]$	Particle conductivity: RBCs
epsilon_p1	50	Particle relative permittivity: platelets
epsilon_p2	59	Particle relative permittivity: RBCs
sigma_s1	$1e-6[S/m]$	Shell electrical conductivity: platelets
sigma_s2	$1e-6[S/m]$	Shell electrical conductivity: RBCs
epsilon_s1	6	Shell relative permittivity: platelets
epsilon_s2	4.44	Shell relative permittivity: RBCs
th_s1	$8[nm]$	Shell thickness: platelets
th_s2	$9[nm]$	Shell thickness: RBCs
dp3	$12[um]$	Particle diameter: White

Table 4.1.: *continued*

Property	Description	Value
sigma_p3	$0.36[S/m]$	Particle conductivity White cells
epsilon_p3	66	Particle relative permitivity: WBC's
sigma_s3	$1e - 6[S/m]$	Shell electrical conductivity: WBC
th_s3	$12[nm]$	Shell thickness: WBC
dp4	$16[um]$	Particle diameter: CTC
sigma_p4	$0.4[S/m]$	Particle conductivity: CTC
epsilon_p4	70	Particle relative permittivity: CTC
sigma_s4	$1e - 6[S/m]$	Shell electrical conductivity: CTC
th_s4	15.5	Shell thickness
epsilon_s4	8	Shell relative permittivity
epsilon_s3	7	Shell relative permittivity
sigma_p5	$0.45[S/m]$	Shell electrical conductivity
epslion_p5	0.5	Shell electrical permittivity
th_s5	$5[nm]$	Shell thickness
th_s6	$4[nm]$	Shell thickness
dp5	$19[um]$	Particle diameter
dp6	$25[um]$	Particle diameter
sigma_p6	$0.45[S/m]$	Shell electrical conductivity
epslion_p6	0.5	Shell electrical permittivity
sigma_s6	$1e - 6[S/m]$	Shell electrical conductivity

The above a parameters are used for the initial simulation of the device. The sizes and other characteristics may vary based on the physical and intrinsic properties of the cells.

4.2.4 Phase 4: Electric Currents Interface

In this phase, the electrical inputs to the electrodes are defined. Since the device is a multistage device, every stage is defined with varied potential. Figure 4.5 depicts the electric insulation of the device, and figure 4.6 shows the applied potential. The charge densities and the electric field are calculated from the equations below:
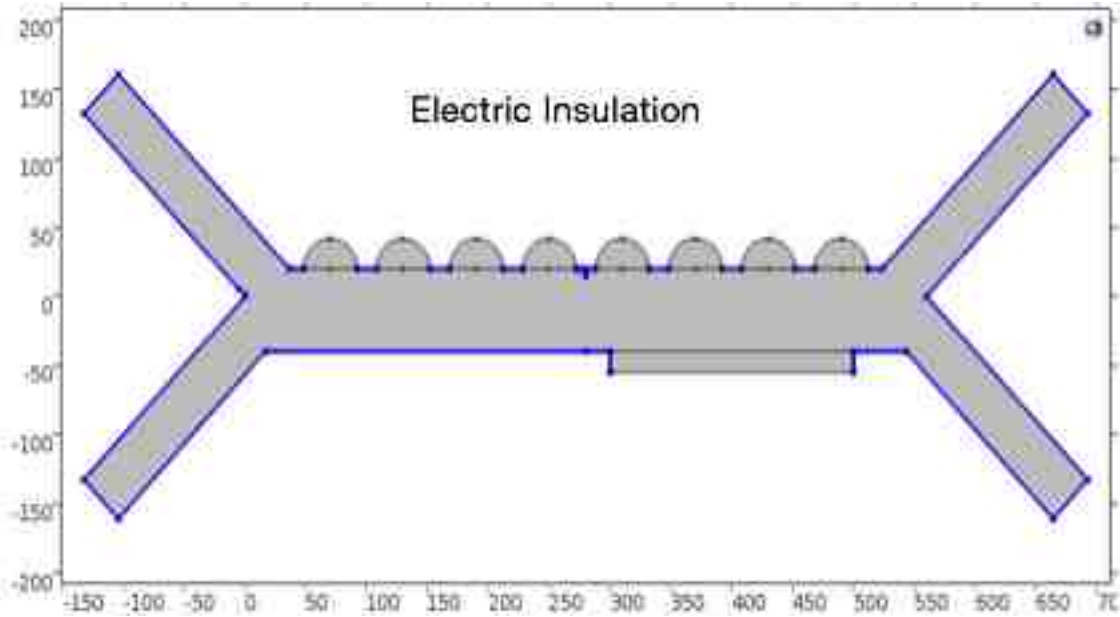
Fig. 4.5. Electric Insulation.

$$\nabla.J = Q + j \tag{4.1}$$

$$J = \sigma_f E + J_e \tag{4.2}$$

$$E = -\nabla v \tag{4.3}$$

The electric field is calculated from the relation,

$$D = \varepsilon_0 \varepsilon_f E \tag{4.4}$$

Where the ε_f is taken from the pre-defined parameters section.
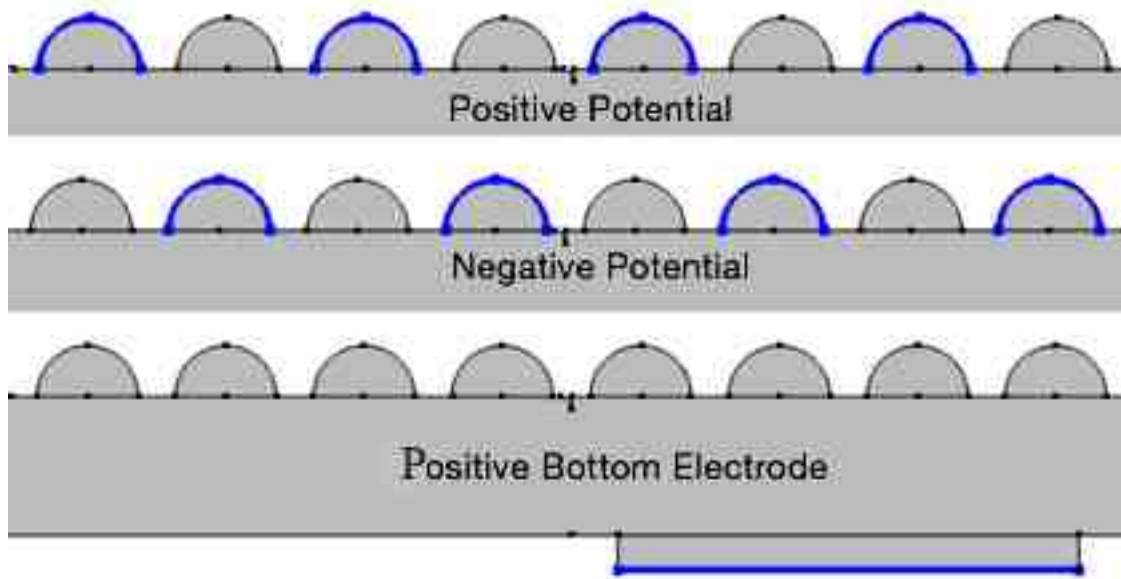
Fig. 4.6. Electrode Boundaries.

4.2.5 Phase 5: Creeping flow Interface

This is the most crucial phase of the design. Since flow parameters cannot be predicted accurately, the design was developed based on some assumptions. Since the flow channels are in micro level, and the Reynolds number is low at this domain creeping flow. This was defined for analyzing the flow characteristics.

This interface calculates the fluid flow based on the following equations of the stationary study analysis.

Flow conditions

$$0 = \nabla. \left[-\rho_f.L + \mu \left(\nabla u + (\nabla v)^T \right) - \frac{2}{3}\mu(\nabla).u)L \right] \tag{4.5}$$

$$\nabla.(\rho_f u_f) = 0 \tag{4.6}$$

Inertial term is neglected due to the low Reynolds number, and the fluid flow is analyzed at 1 atm reference pressure. For the ideal simulation, we assumed the wall boundary condition as a non-slip and used an elemental constraint method. While defining the inlet velocities as a normal inflow velocity is assumed for the simulation.

Fluid Wall boundary conditions

The interaction of the fluid with the wall of the microfluidic channel is a crucial factor. Since the device is small and the channel may block, leading to the leakages in the device, initially no slip conditions was used for simulating device for accurate results. Fluid velocity and pressure were analyzed for various other wall boundary conditions.

Slip condition:

$$K - (K.n)n =, K = \left[\mu(\nabla u) + (\nabla u)^T) - \frac{2}{3}\mu(\nabla.u)l \right] n \tag{4.7}$$

No Slip condition:

$$u = 0 \tag{4.8}$$

Sliding wall:

$$u = U_w t \tag{4.9}$$

Leaking wall:

$$u = u_w \tag{4.10}$$

Electroosmotic velocity:

$$u = \mu_{e0} E_t, E_t = E - (E.n)n \tag{4.11}$$

Slip velocity:

$$u = u_w \tag{4.12}$$

4.2.6 Phase 6: Particle Tracing Interface

This is the key phase which concentrates on the aim of the project. This interface solves the particle movement in microfluidic channel considering electric potential and dielectrophoretic force on each and every particle. This interface is computed dynamically based on the time dependent study. Particle's physical characteristics play a important role in determining the movement in fluidic channel.

Particle analysis

The model is studied based on the following equations:

$$F_t = \frac{d(m_p v)}{dt} \tag{4.13}$$

The temperature of the particle is given by:

$$m_p C_p \frac{dT_p}{dt} = h A_p (T - T_p) \tag{4.14}$$

the final temperature of the cell may be obtained as a result of the heat lost to the fluid or gained from the fluid and it is a function of time.

$$R = \frac{dm_p}{dt} \tag{4.15}$$

Particle wall Interactions

Studying the particle and fluid interaction with the wall of the microfluidic channels is one of the key factors that needs to be considered while designing the device. Various particles in the blood may exhibit different type of interactions with the wall. This system is solved for a bouncing wall-particle boundary conditions. The physics solved for the various particle wall boundary conditions are given below:

Bounce:

$$n = v_{pw} - 2(n.v_{pw})n \tag{4.16}$$

Freeze:

$$v = v_{pw} \tag{4.17}$$

Stick:

$$v = 0 \tag{4.18}$$

Disappear:

$$q = NaN \tag{4.19}$$

Diffuse Scattering:

$$v_t = |v_{pw}|sin(\theta) \tag{4.20}$$

$$v_n = |v_{pw}|cos(\theta) \tag{4.21}$$

Mixed Diffuse and specular reflection:

$$n = v_{pw} - 2(n.v_{pw})n \tag{4.22}$$

$$v_t = |v_{pw}|sin(\theta) \tag{4.23}$$

$$v_n = |v_{pw}|cos(\theta) \tag{4.24}$$

General scattering occur at the conditions where:

$$v_n = v_{pw} \tag{4.25}$$

Drag force

Since drag forces plays a major role in microfluidic devices, the following formulations are computed to calculate the drag force on a particle.

$$F = \frac{1}{\tau_p}m_p(u - v) \tag{4.26}$$

$$\tau_p = \frac{\rho_p d_p^2}{18\mu_f} \tag{4.27}$$

Dielectrophoretic force formulations are based on the equations discussed in chapter 3. This finishes the designing of the device.

4.2.7 Phase 6: Meshing
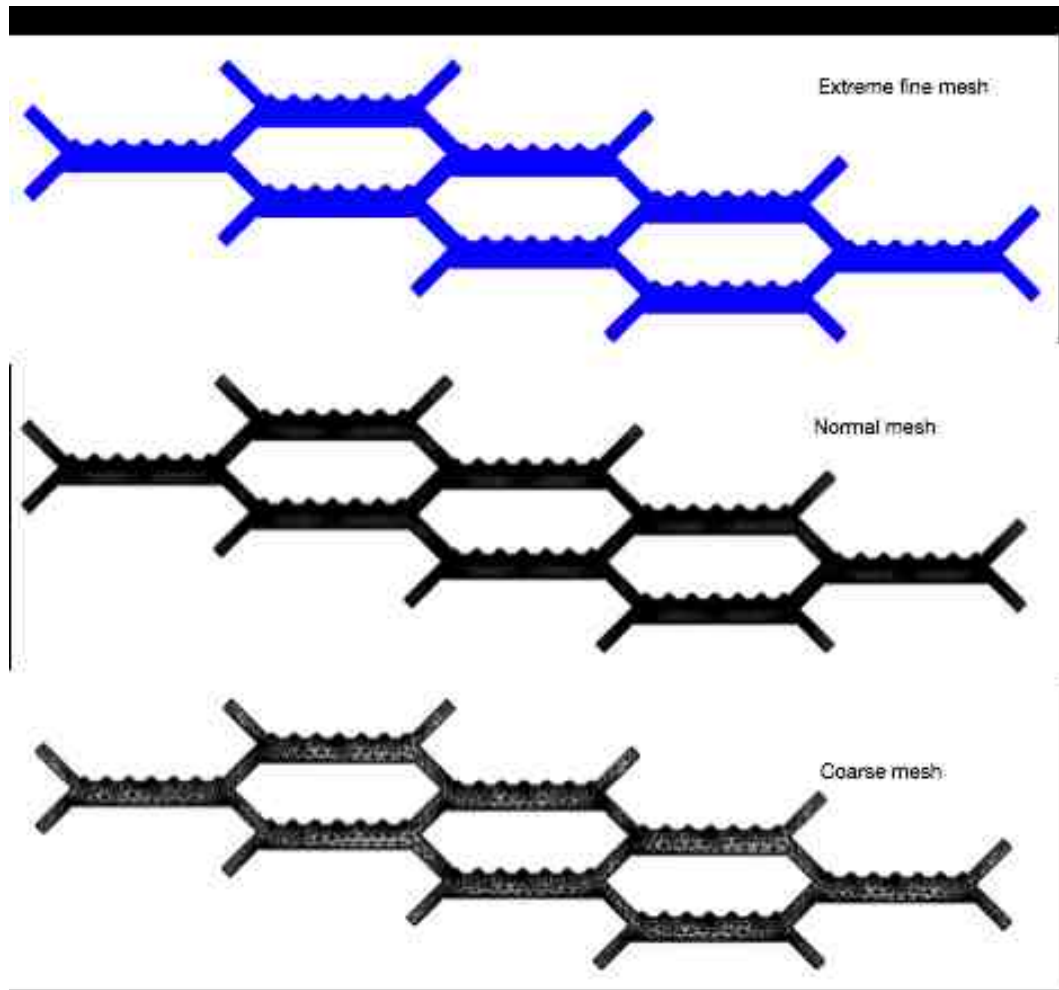
Fig. 4.7. Mesh types.

5. RESULTS AND DISCUSSION

After modelling the device, the analysis of the device is done in two stages. In the first stage the electric potential and the creeping flow were computed. In the second phase, time dependent particle flow module is calculated.

5.1 Study 1: Electric and Fluid Flow Analysis

Initial study is further computed. Initially a frequency domain analysis for the electric field analysis and a stationary analysis for the fluid flow was estimated with the physics defined in electric currents and creeping flow interfaces.

5.1.1 Stationary Study

Since the voltage is constant over the time, stationary study is used. This study is used to analyze and compute static electric and magnetic fields. In fluid flow stationary study is used to compute the steady flow and pressure fields in channels.

5.1.2 Frequency Domain Analysis

This study is used to compute and analyze the linear or linearized models subjected to harmonic excitation for one or several frequencies. Electromagnetics theory is used to compute the transmission and reflection versus frequency.

5.1.3 Time Dependent Analysis

This study is used when the variables in the formulation changes overtime. In fluid flow, it is used to analyze the unsteady flow and pressure fields generated in

the channels. In particle flow interface, this study is used to analyze the movement of a cell in electric and fluids flowing microfluidic medium. Particles are released in specific time intervals. The model is simulated for 2 cells, 4 cells, 6 cells and in various combinations based on their average population ratio.

5.2   Results

(a) Electric Field X Component $\frac{V}{m}$.

(b) Electric Field Y Component $\frac{V}{m}$.
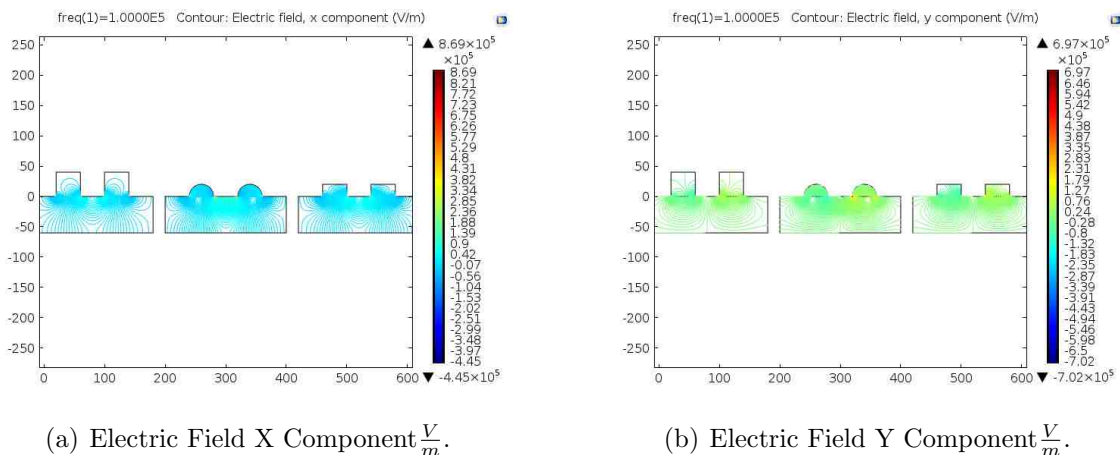
Fig. 5.1. Surface: Electric Field Contour Plot.
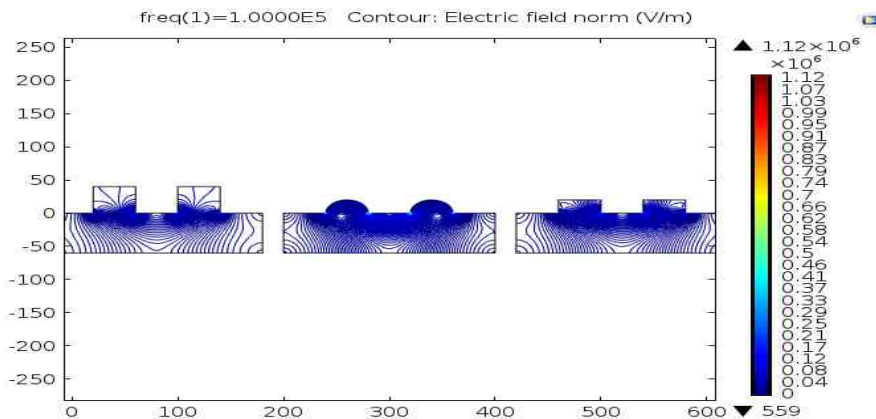
Fig. 5.2. Surface: Electric Field Norm Component.

(a) Electric Displacement Field X Component $\frac{V}{m}$.

(b) Electric Displacement Field Y Component $\frac{V}{m}$.
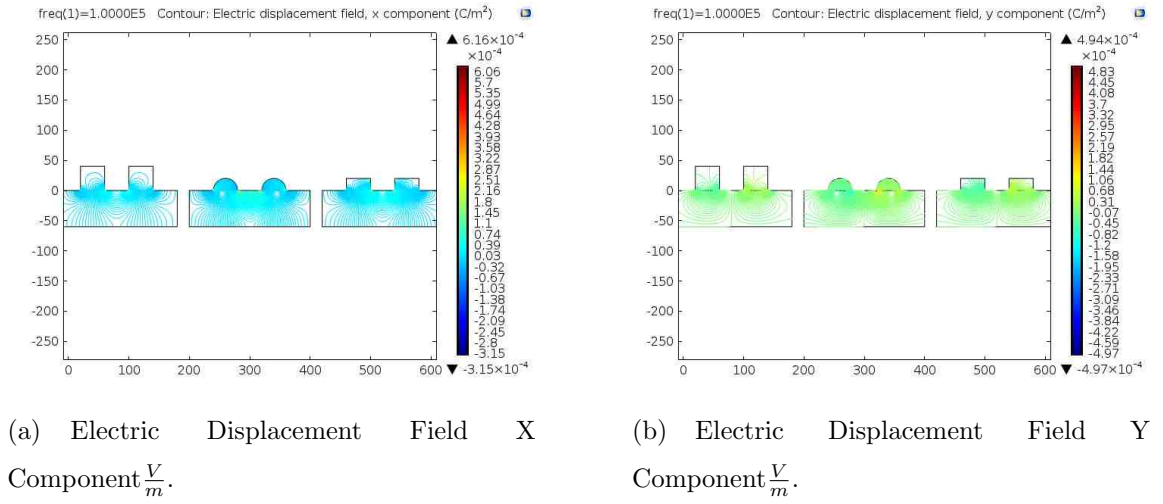
Fig. 5.3. Surface: Electric Displacement Field Contour Plot.
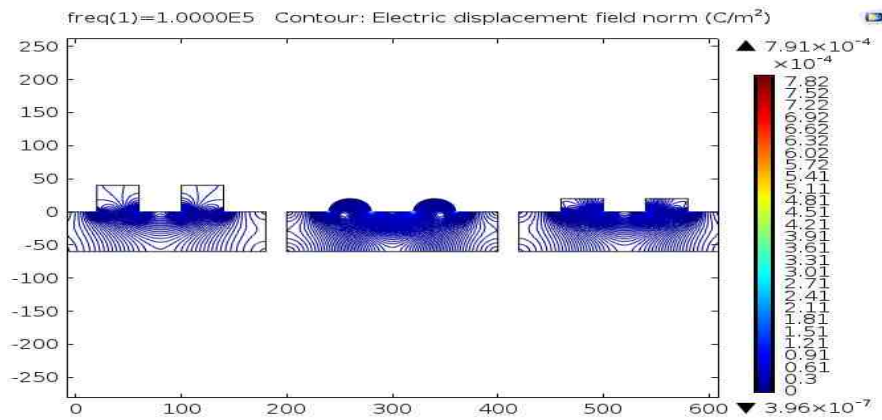
Fig. 5.4. Surface: Electric Displacement Field Norm Component.

(a) Polarization X Component $\frac{V}{m}$. (b) Polarization Y Component $\frac{V}{m}$.
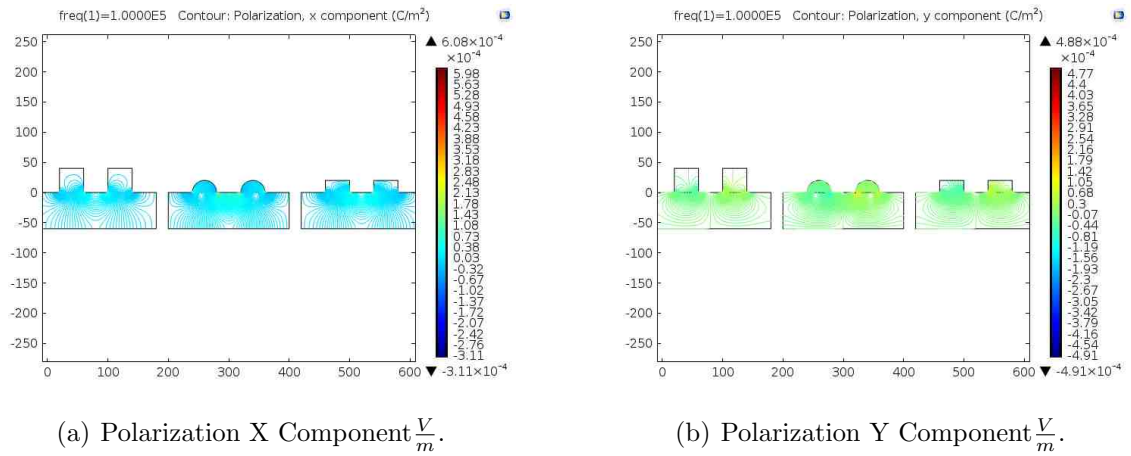
Fig. 5.5. Surface: Polarization Contour Plot.

Fig. 5.6. Surface: Polarization Norm Component.
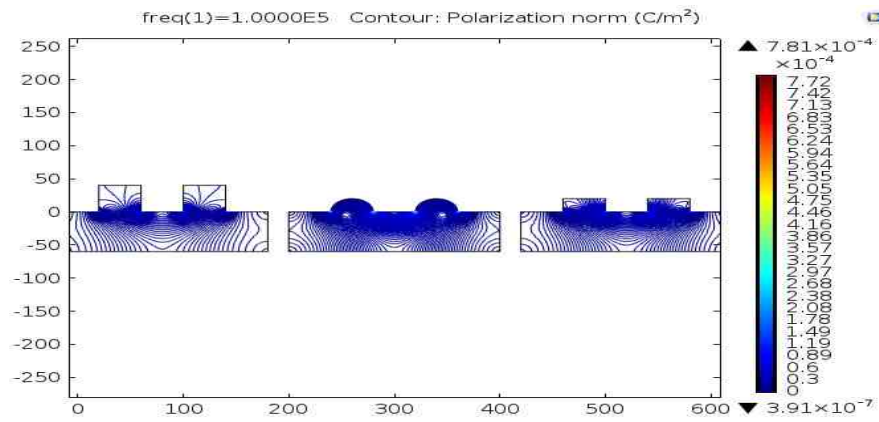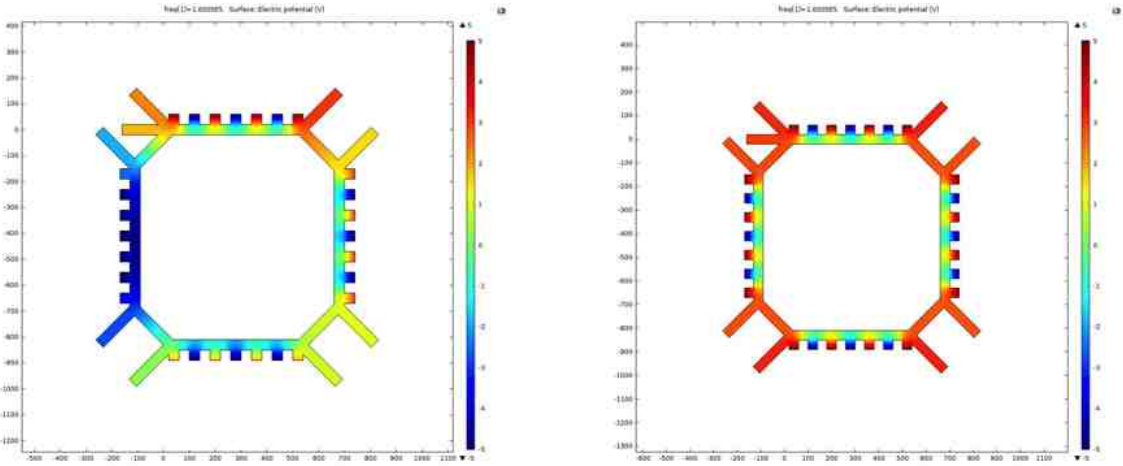
(a) Variable Potential: Velocity Magnitude($\frac{m}{sec}$).

(b) Uniform field: Velocity Magnitude.

Fig. 5.7. Electric Current: Electric Potential of Quadruple Circular Cell Sorter.
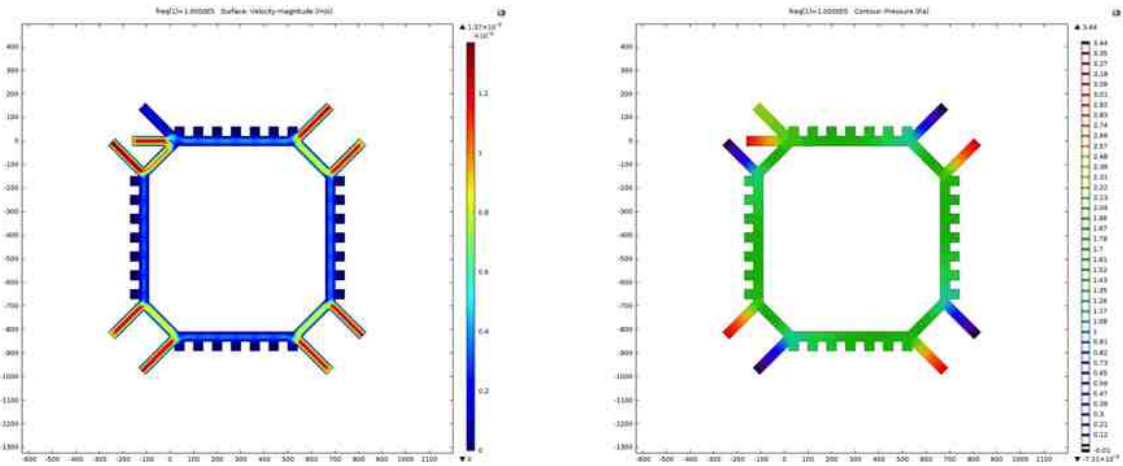
(a) Surface: Velocity Magnitude($\frac{m}{sec}$).

(b) Contour: Pressure (Pa).

Fig. 5.8. Creeping flow: Uniform field Quadruple Circular Cell Sorter.
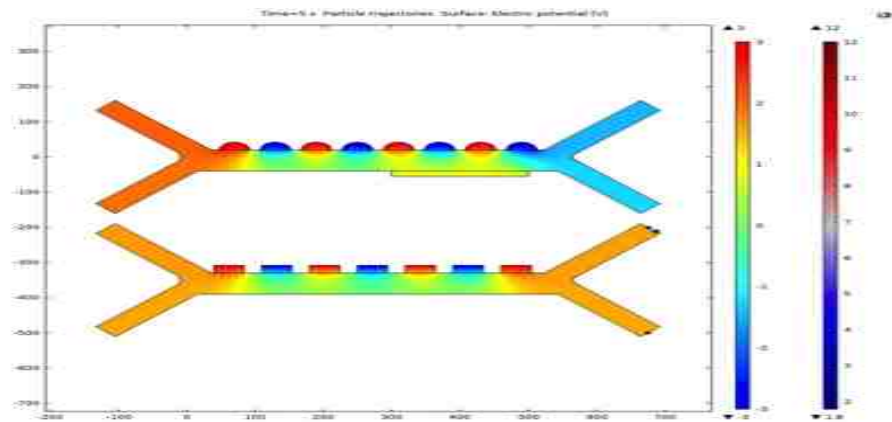
Fig. 5.9. Electric Current: Electric Potential -Semi-Circular Electrode vs Rectangular Electrodes.
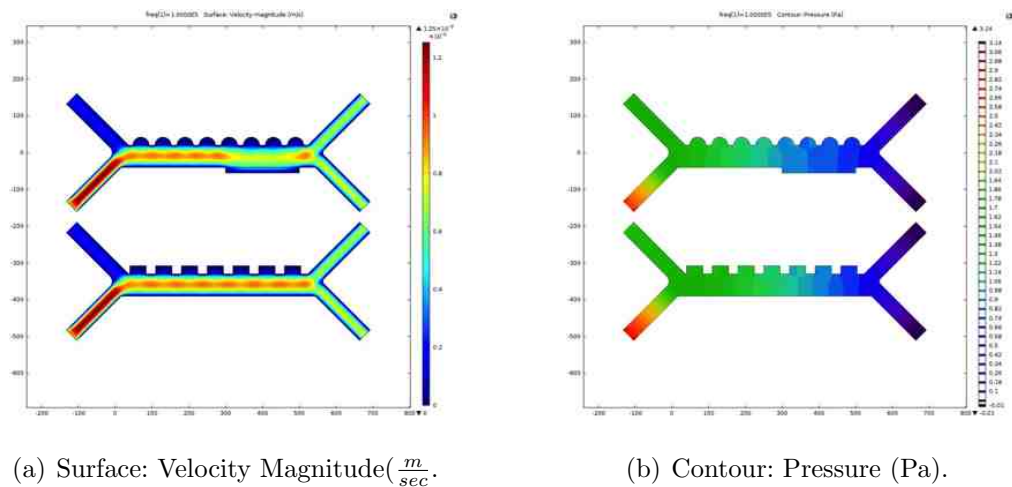
(a) Surface: Velocity Magnitude($\frac{m}{sec}$.

(b) Contour: Pressure (Pa).

Fig. 5.10. Creeping flow: Semi-Circular Electrode vs Rectangular Electrodes.
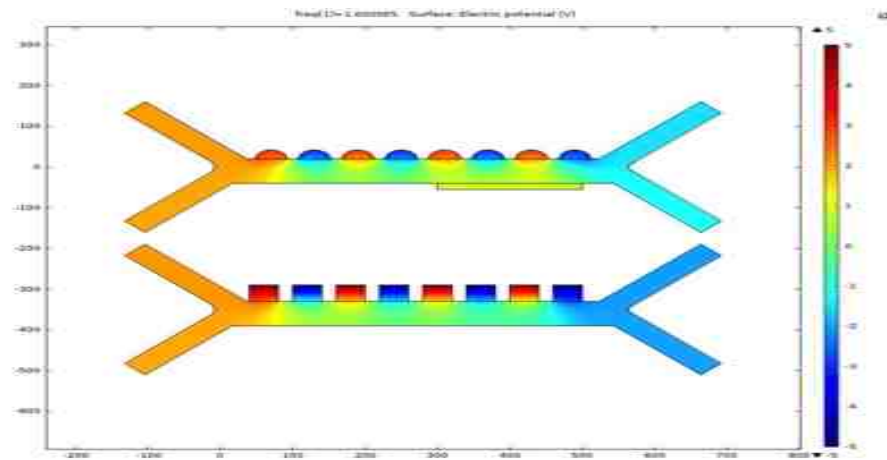
Fig. 5.11. Electric Current: Electric Potential-Semi-Circular Electrode vs Rectangular Electrodes.
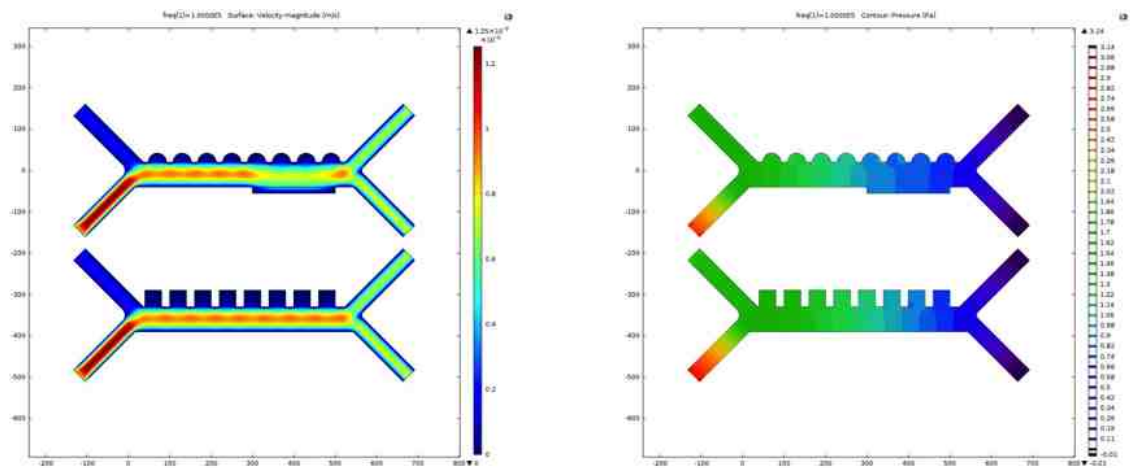
(a) Surface: Velocity Magnitude($\frac{m}{sec}$).

(b) Contour: Pressure (Pa).

Fig. 5.12. Creeping flow: Semi-Circular Electrode vs Square Electrodes.
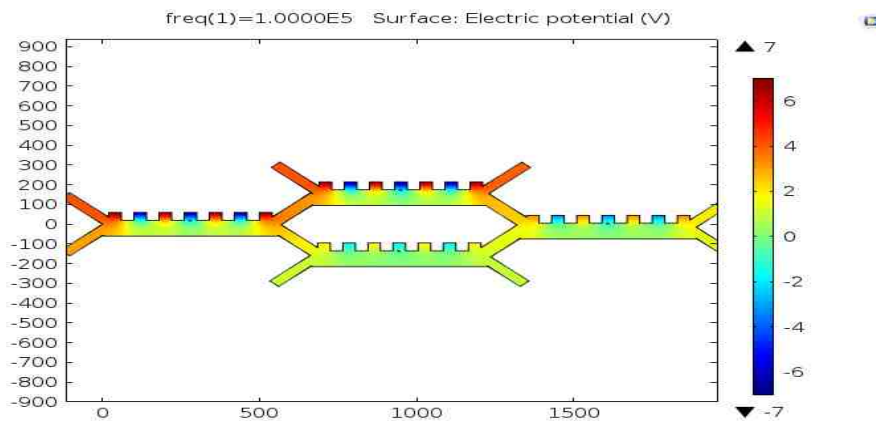
Fig. 5.13. Rectangular Electrode: Electric Potential four Cell sorter.
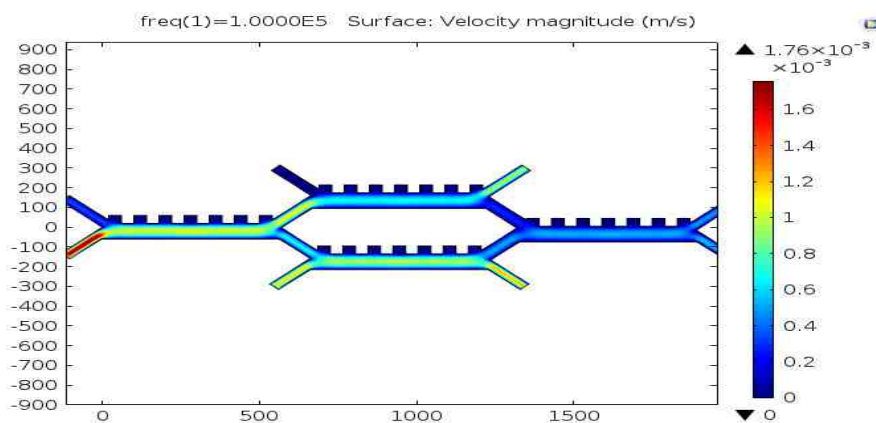
Fig. 5.14. Rectangular Electrode Creeping Flow: Velocity four cell sorter.
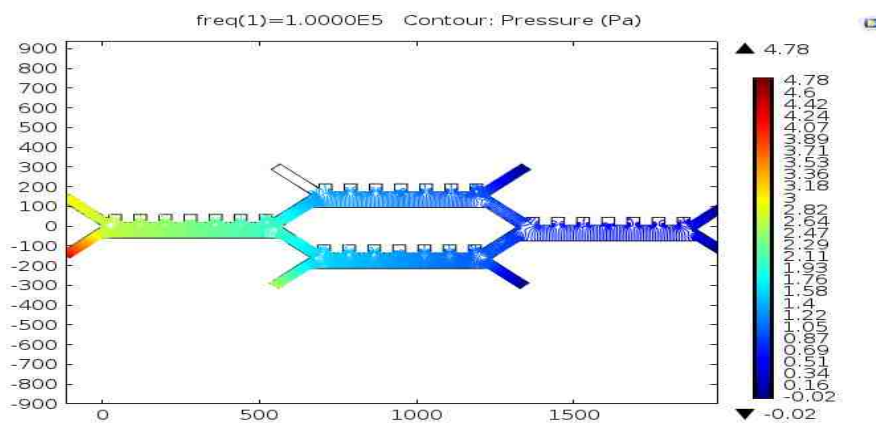
Fig. 5.15. Rectangular Electrode Creeping Flow: Pressure four cell sorter.
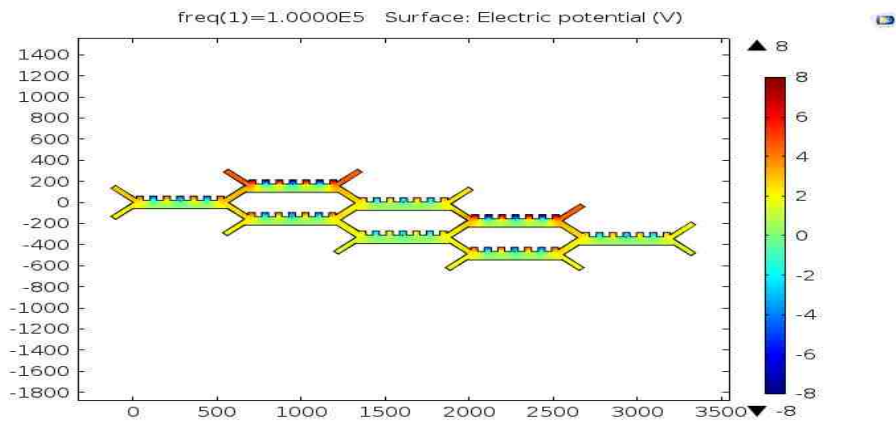
Fig. 5.16. Rectangular Electrode: Electric Potential.
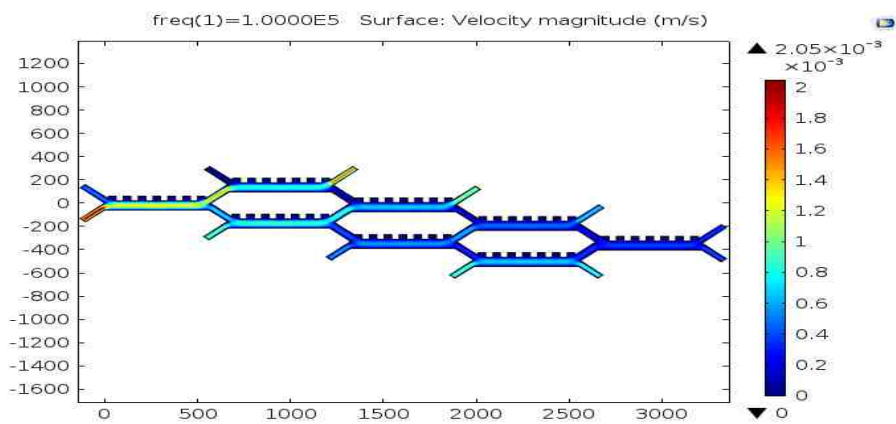
Fig. 5.17. Rectangular Electrode Creeping Flow: Velocity.
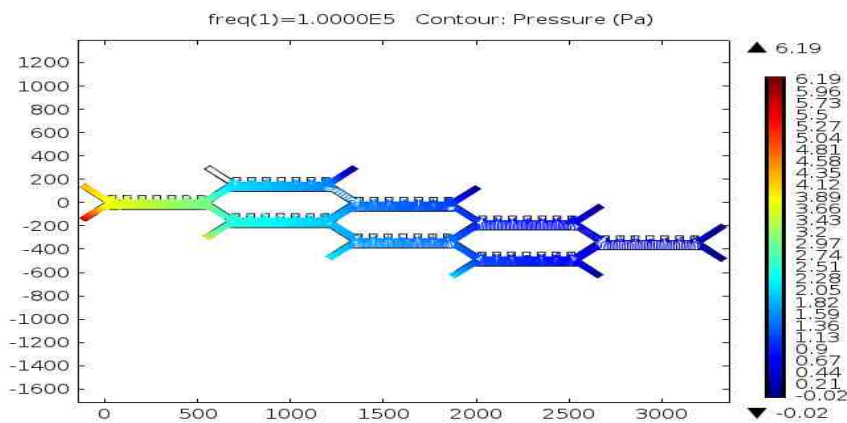
Fig. 5.18. Rectangular Electrode Creeping Flow: Pressure.

5.2.1 Six Cell Sorter-Semicircular Electrodes
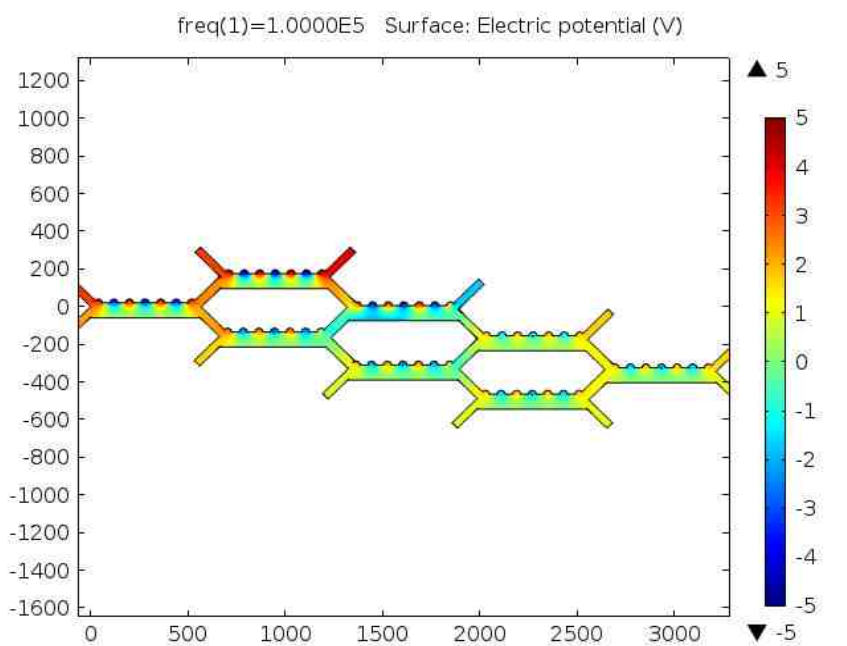
Fig. 5.19. Semi-Circular Electrode: Electric Potential.
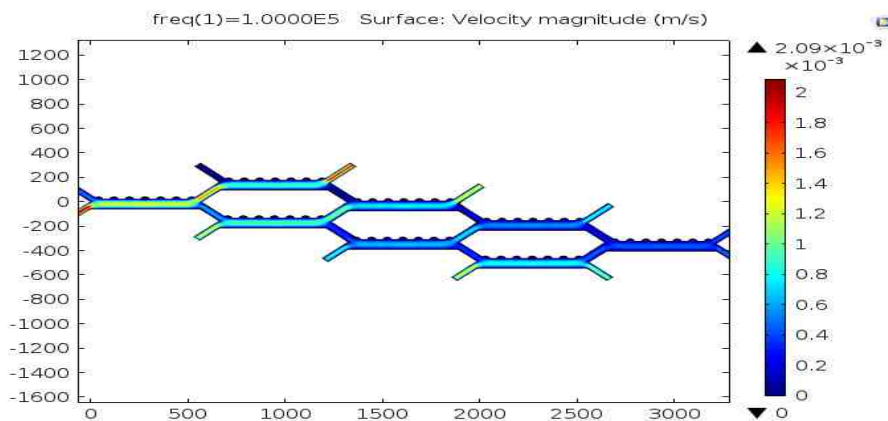
Fig. 5.20. Semi-Circular Electrode Creeping Flow: Velocity.
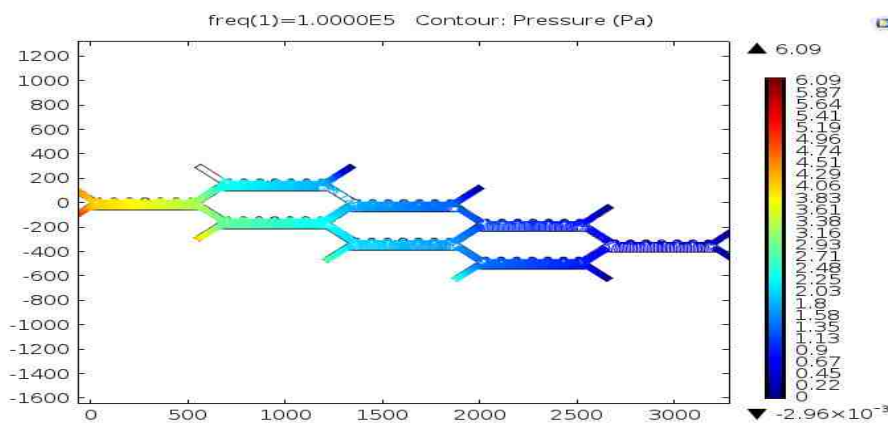
Fig. 5.21. Semi-Circular Electrode Creeping Flow: Pressure.

5.2.2   Issues With Cell Sorting During Simulation

Due to the lower electrode potential the cells are not influenced by weaker electrical fields and due to higher electric fields the cells were pushed towards the lower wall and leads to clogging of channel. Below figures shows the various cases that were to be taken care while developing a cell sorting device. Figure 5.20 shows the cells exiting out through the upper outlet and figure 5.23 depicts all the cells passing through the lower outlet. To avoid this a medium electrode potential is required in order to attain a efficient sorting of the cells.
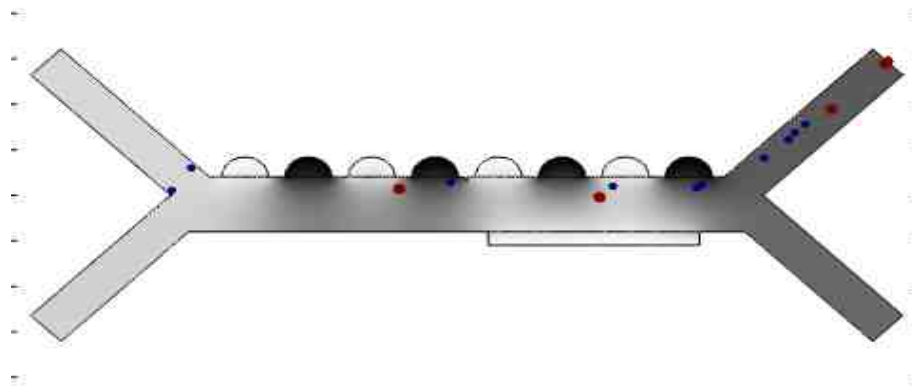
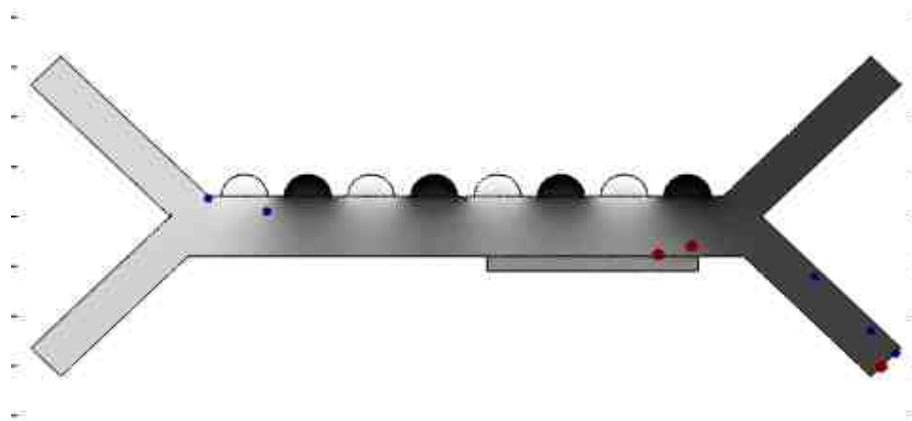Fig. 5.22. Sorting Issues: Lower Electrode potential.

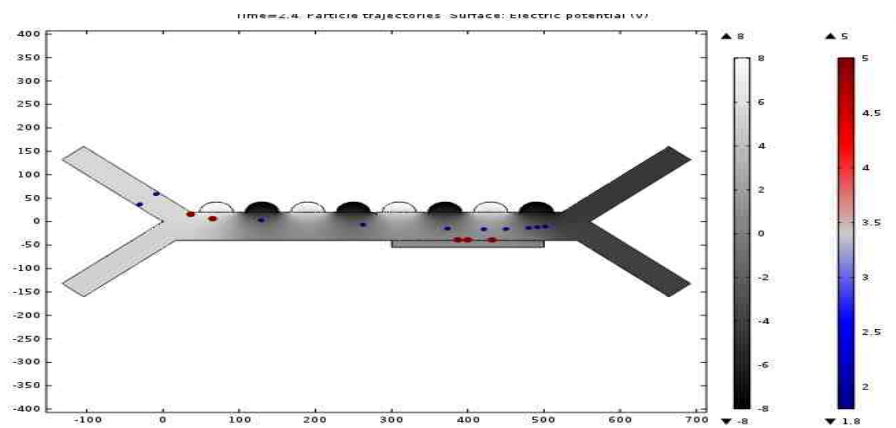Fig. 5.23. Sorting Issues: Higher Electrode potential.

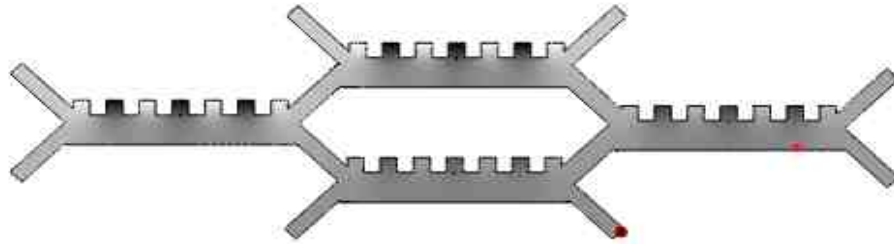Fig. 5.24. Sorting Issues: Higher Electrode potential and Cell Sticking to Walls.
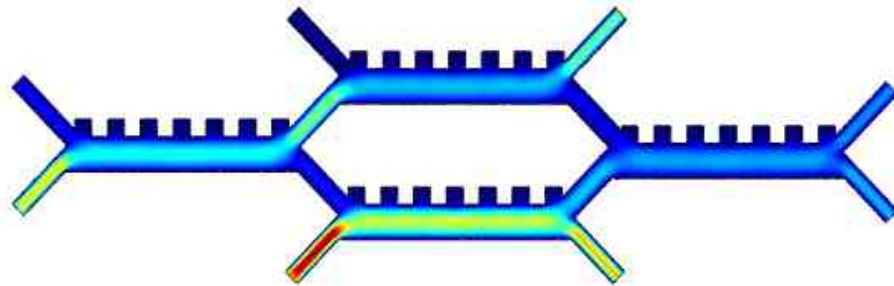
Fig. 5.25. Efficient Sorting Path.

Fig. 5.26. Sorting Issues: Higher Velocity.

Figure 5.25 shows the assumed path of the cells. Below figure shows the effect of potentials and velocities in deviation of cell paths.

These issues were solved by defining the exact potentials and velocities using the values from the numerical models that were solved in Chapter 3.
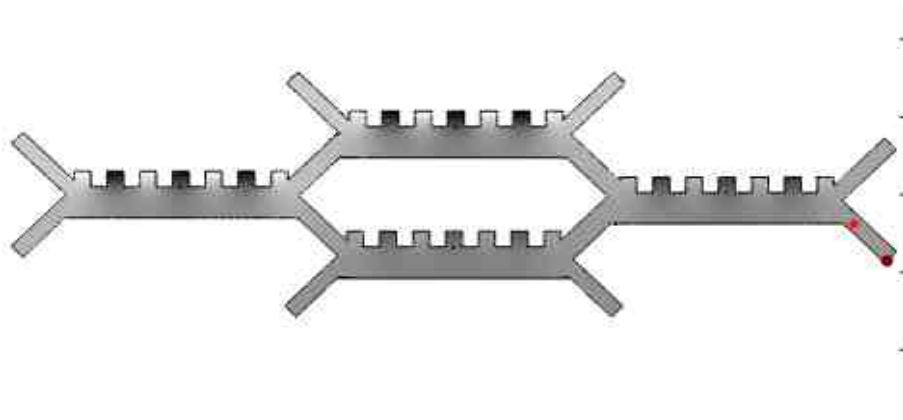
Fig. 5.27. Sorting Issues: Lower Electrode Potential Resulting Deviated Paths.
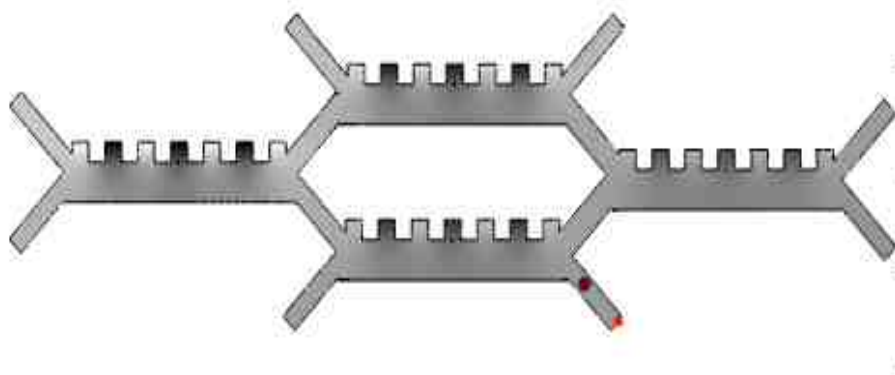

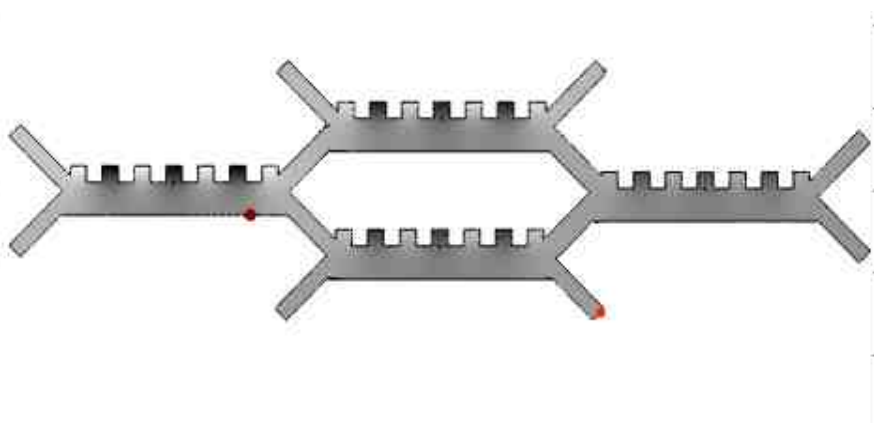Fig. 5.28. Sorting Issues: Higher Potential Resulting Deviated Paths.

Fig. 5.29. Sorting Issues: Deviated Potential and Velocity Resulting Sticking and Deviated Paths.

6. DEVELOPMENT OF MEMS USING 3D PRINTING

3D printing, called stereolithography, is used to demonstrate the proposed model. The slices are selected in such a away that it selectively chooses the harden layer of liquid which is sensitive to the ultra violet radiation to achieve the designed shape. The model was printed layer by layer, and after each layer is made, the building platform is lowered by a fraction, and the process of printing is repeated until the model is completed.

Several alternatives and inspired techniques have been evolved since the invention of the stereolithography. Laser sintering method prints the powdered plastic, metal or resins with a laser beam to harden the deposit in specified places excluding others to achieve the physical model. Some other processes uses electric beam instead of UV light. Some processes melts metallic powder as it is deposited on the model. This is used to weld the parts as well as repair the damaged parts with sensitive design parameters like turbine blades. Some 3D printers operates similar to the 2D inkjet printers, printing the photo-sensitive liquid layer by layer further strengthening or hardening them.

Among all the modeling techniques the fused deposition modeling, which is achieved by a computer-controlled glue gun. In this process a heated nozzle extrudes a filament of thermoplastic, which hardens as it cools.

6.1   3D Model and Software

The Prototype of the simulated model is modelled by maximizing it 1000 times the original design. The 3D model is modeled in PTC Creo Parametric 2.0.

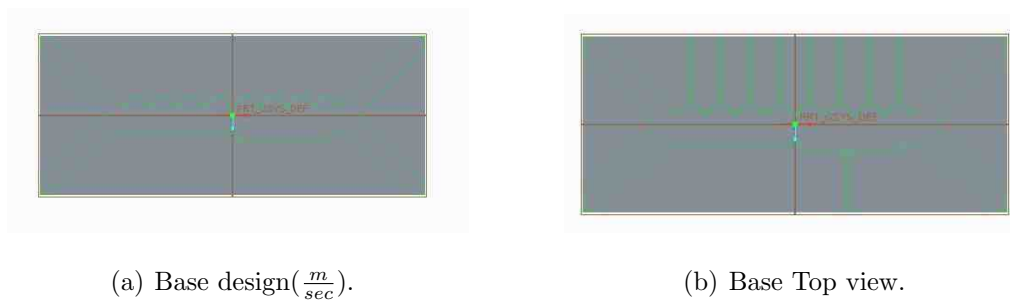(a) Base design($\frac{m}{sec}$).

(b) Base Top view.
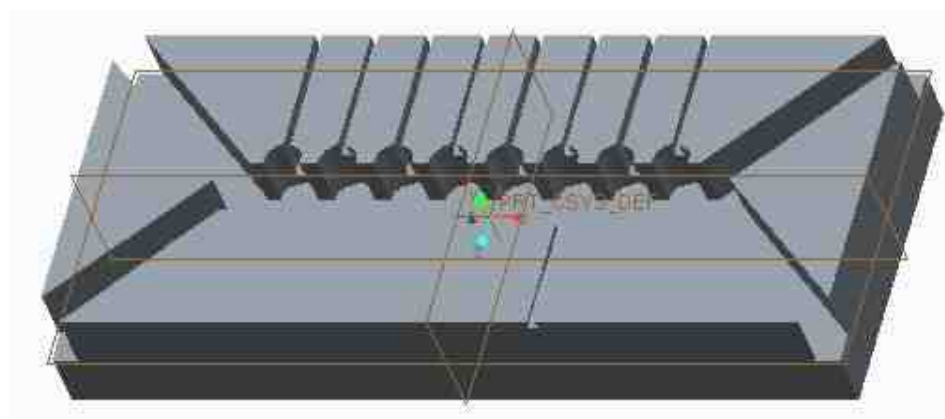
Fig. 6.1. Microfluidic Cell Sorter Base Design.
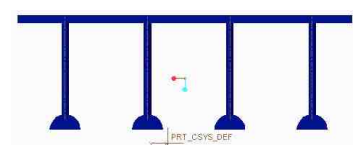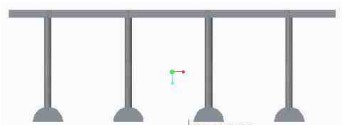

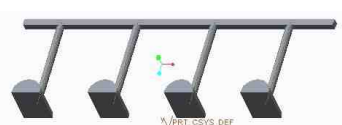Fig. 6.2. 3D View: Microfluidic Cell Sorter Design.

(a) Top View: Negative Electrode.

(b) 3D View: Negative Electrode.

(c) Top View: Positive Electrode.

(d) 3D View: Positive Electrode.

Fig. 6.3. Electrode Modeling and Design.

Fig. 6.4. Top View: Microfluidic Cell Sorter Design.
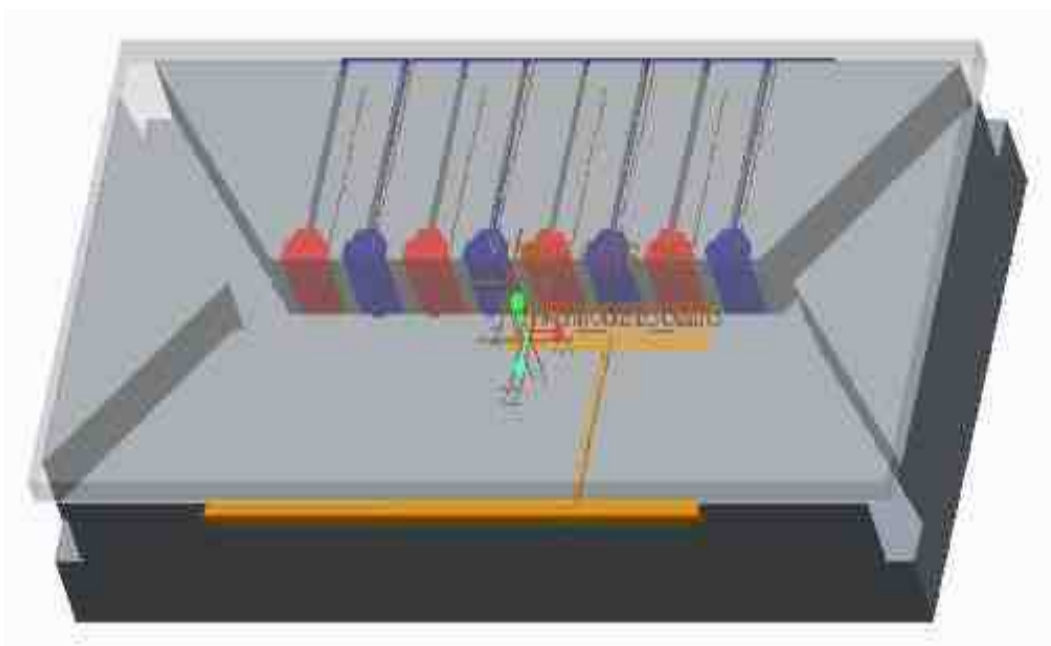
Fig. 6.5. 3D View: Microfluidic Cell Sortor Design.
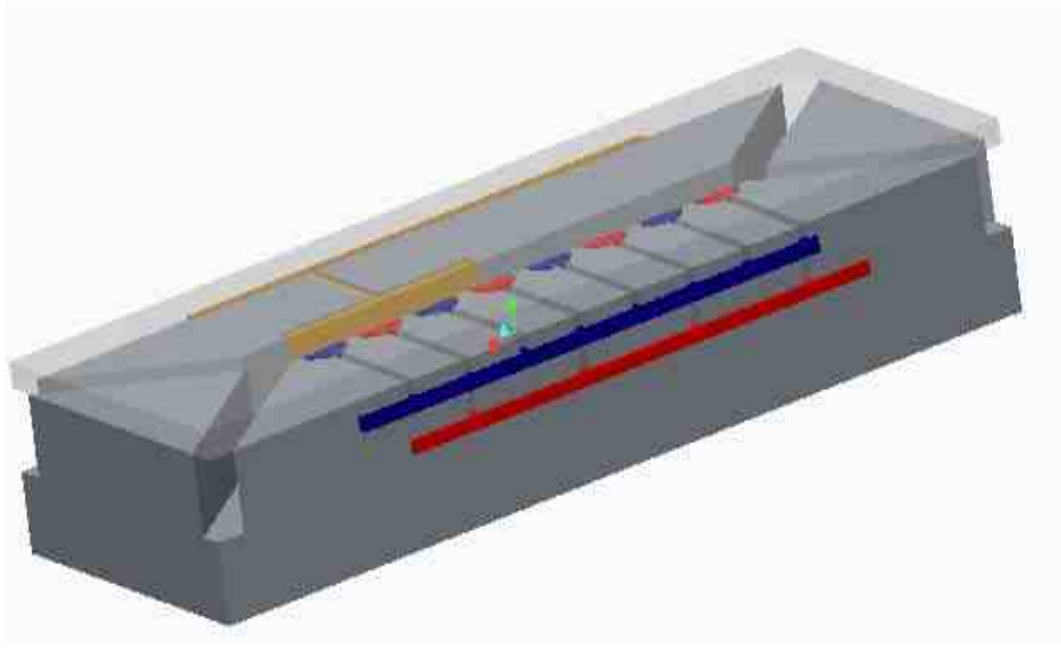
Fig. 6.6. 3D View: Microfluidic Cell Sortor Design Electrode Assembly.

6.2   Prototype Model Design

The prototype model is built through the help of Sculpteo 3D building company. The stereolithography files were created from the COMSOL and PTC Creo tools for building the 3D model. Below are the figures that shows the various prototype models depicting the channel structure the electrode layout and the multi layer devices.
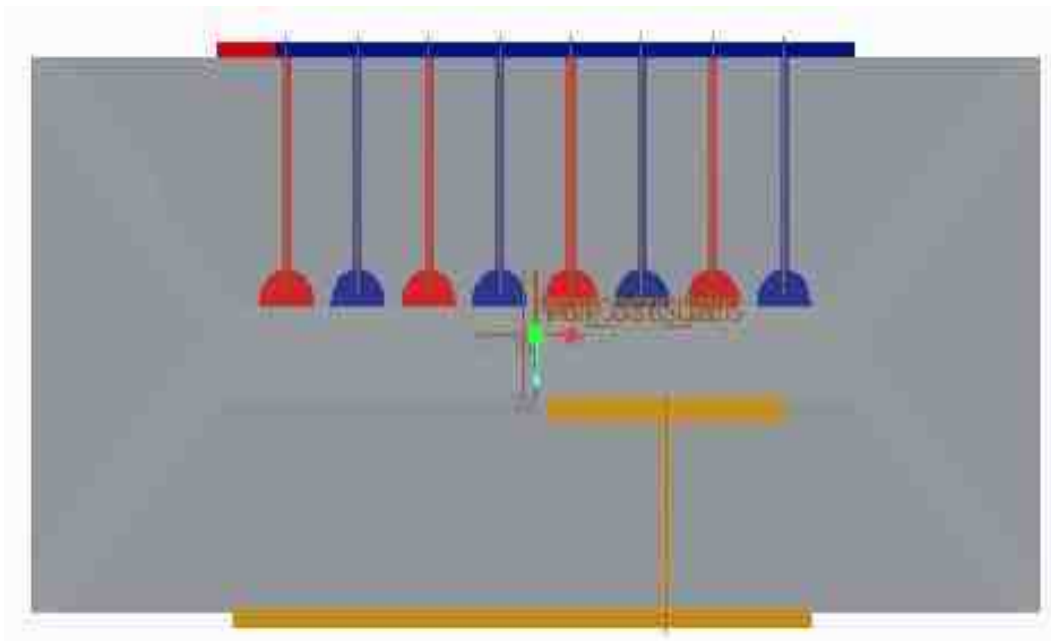
Fig. 6.7. 3D Channel View: 6 Microfluidic Cell Sorter Design.

Fig. 6.8. 3D Top View: Microfluidic 6 Cell Sorter Design.

Fig. 6.9. COMSOL3D View: Microfluidic Cell Sorter Design Channel View.
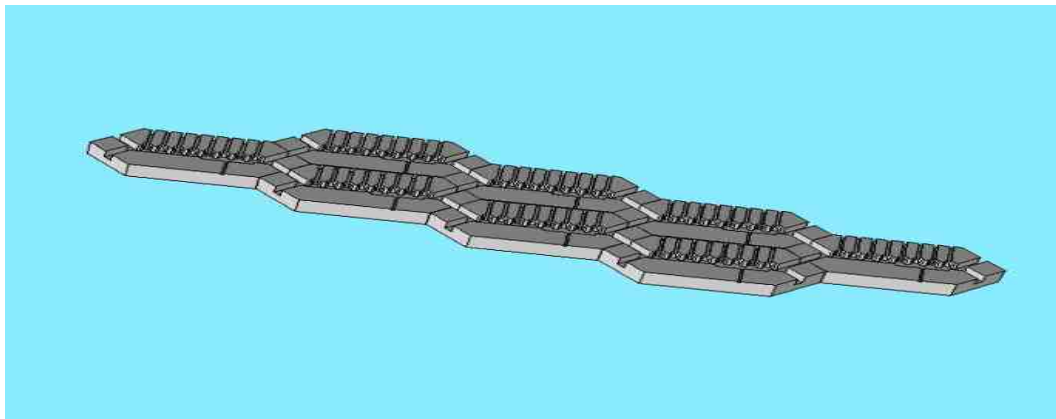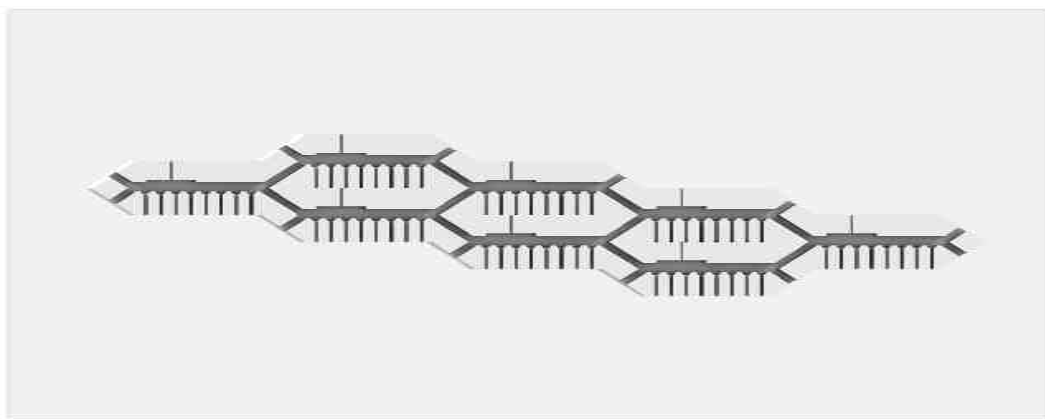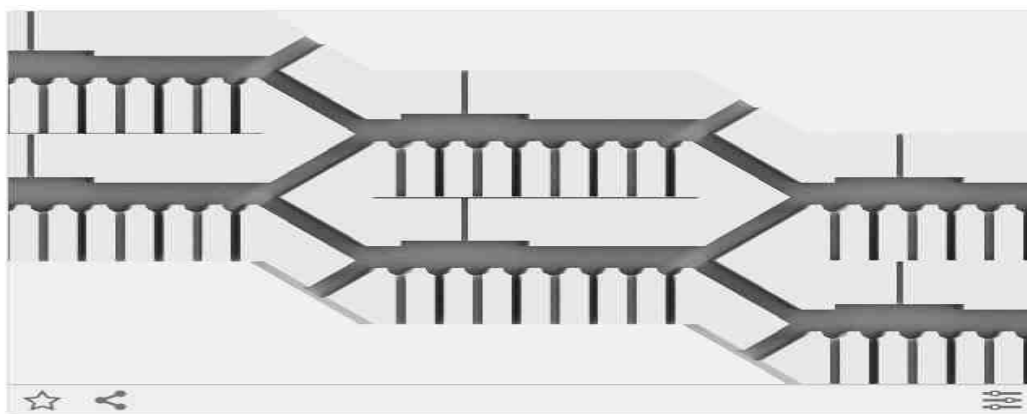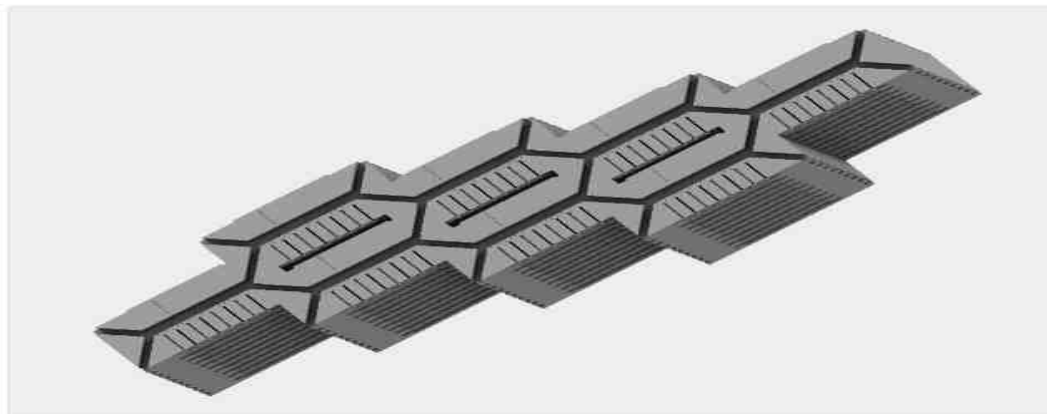
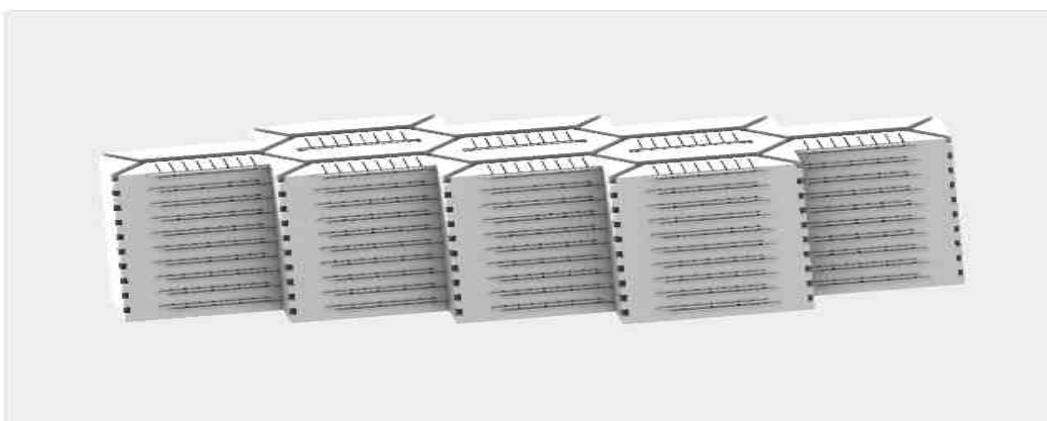Fig. 6.10. COMSOL3D View: Stacked Microfluidic Cell Sorter Design.

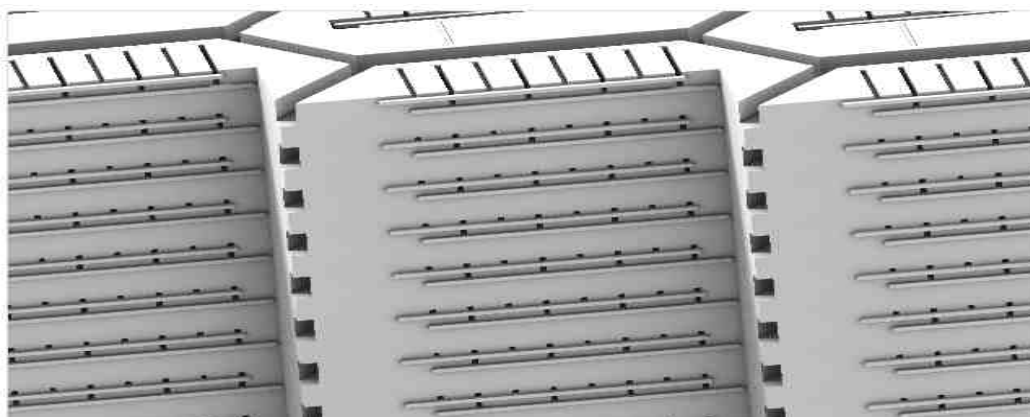Fig. 6.11. 3D Side View of Microfluidic Cell Sorter Design With Electrode Connections.

Fig. 6.12. COMSOL 3D: Electrode Connections View.

7. CONCLUSION AND FUTURE WORK

In this research we have successfully developed the software model for manipulating the human blood cancer cells within multistage microfluidic channels using COMSOL Multiphysics software. The approach utilizes magnetic field forces, followed by electric field manipulation via different electrode potentials within the channels. The design has successfully proved the concept that with a low voltage electrode potential applied to microfluidics the required electric field needed for the cell separation has been achieved. The system utilizes spherical electrodes for achieving high electric field by low electrode potentials applied to human blood cells. As low as 5V electrode potential for the rectangular electrode and 3V for the semi sphere electrodes have led to the cell separation within 60 m diameter size channel. An ac electrode potential of 100 KHz was used, to better steering the cells within the channel. The ac field was important to avoid the formation of debye layer effect, and more appropriate to incorporate the complex relative permittivity of the cells.

The feature of the minimum power consumption of this system may result in a high probability of cancer cell survival within the separation process inside the cascaded stages of the microfluidic system. This makes it appropriate for the MRD (minimum residual disease) application that may lead to the early detection and diagnosis of human blood cancer. The critical parameters of the channel length, the speed of the blood flow, the location of the electrodes throughout the channels, and the timing diagram for the electrode potentials is of large impact on the process. The process and synchronization activities were handled by the software, however, for future consideration, a control unit must be considered to synchronize the activities among the various units of the system, including the flow speed, the electrode potentials, among other feedback of the system components. The proper values of the device parameters have been verified by tracking failure cases when altering these parameters.

For instance, the simulation results have showed failure separation when the velocity is slower than the estimated value from simulation, and other cases when the field strengths were higher that the suggested values from simulation. In these cases, the cells were observed to be sticking by the channel walls and unable to progress with the separation process. In such cases, cells may take different paths and affect the sorting process.

The integrated development of the fluid mechanics and electromagnetics, together with the particle tracing, has led to a full characterization of the blood separation process, in particular with the accurate model developed here to incorporate aspects from electrical, magnetic, physical, mechanical, deformity, alignment, and biological properties into the integrated model. Furthermore, the model addresses the scalability of the device for future practical applications. Overall, the proposed system features portability, reliability, accuracy, high speed, and low cost.

Due to the nonlinear models and the complexity of the device system, practical models may deviate from the ideal model, suggesting some minor modification to the parameters will be needed. The minor deviation of the practical model from the simulation model suggests a calibration process, determining the exact velocity in relative to the device parameters. In this case, the control unit will be programmed to provide the proper parameters to activate electrodes and synchronize the device activities.

Within an ideal setup model, the system has provided near 100% cancer blood cell separation from normal cells. With minor modifications to the research parameters, including channel length, flow speed, channel size, electrical potential distribution, and mechanical structure of the channels, the system may be extended to other types of cancers such as colon, liver, etc., where sorting and counting will be achievable.

Since the PH of the blood cell and other protein/fat/composition in the blood, the separation process may be also applied to other application such as LDL/HDL protein separation, a process that may competing with the LDL apheresis process. The microfluidic structure may take either the rectangular or circular cross-sectional

device systems. In the later, a coaxial multistage or conical configuration may be appropriate to separate the cancer cells from the normal ones. The field nonlinearity of the conical structure may assist with the separation.

REFERENCES

REFERENCES

[1] A. R. Wheeler, W. R. Throndset, R. J. Whelan, A. M. Leach, R. N. Zare, Y. H. Liao, K. Farrell, I. D. Manger, and A. Daridon, "Microfluidic device for single-cell analysis," *Analytical Chemistry*, vol. 75, no. 14, pp. 3581–3586, 2003.

[2] P. K. Horan and L. L. Wheeless, "Quantitative single cell analysis and sorting," *Science*, vol. 198, no. 4313, pp. 149–157, 1977.

[3] R. Ruddon and E. Inc., *Cancer Biology.* 3rd Edition, Oxford University Press, New York, 2007.

[4] A. Jemal, R. Siegel, J. Xu, and E. Ward, "Cancer statistics, 2010," *CA: A Cancer Journal For Clinicians*, vol. 60, no. 5, pp. 277–300, 2010.

[5] A. R. Wheeler, W. R. Throndset, R. J. Whelan, A. M. Leach, R. N. Zare, Y. H. Liao, K. Farrell, I. D. Manger, and A. Daridon, "Microfluidic device for single-cell analysis," *Analytical chemistry*, vol. 75, no. 14, pp. 3581–3586, 2003.

[6] D. Anselmetti, *Single Cell Analysis.* Hoboken:Wiley, 2009.

[7] D. G. Iorgulescu and G. K. Kiroff, "Minimal residual marrow disease: detection and significance of isolated tumour cells in bone marrow," *ANZ Journal of Surgery*, vol. 71, no. 6, pp. 365–376, 2001.

[8] H. C. Engell, "Cancer cells in the circulating blood; a clinical study on the occurrence of cancer cells in the peripheral blood and in venous blood draining the tumour area at operation," *Ugeskrift for Laeger*, vol. 117, no. 25, pp. 822–822, 1955.

[9] A. Armakolas, Z. Panteleakou, A. Nezos, A. Tsouma, M. Skondra, P. Lembessis, N. Pissimissis, and M. Koutsilieris, "Detection of the circulating tumor cells in cancer patients," *Future Oncology*, vol. 6, no. 12, pp. 1849–1856, 2010.

[10] V. Zieglschmid, C. Hollmann, and O. Böcher, "Detection of disseminated tumor cells in peripheral blood," *Critical reviews in Clinical Laboratory Sciences*, vol. 42, no. 2, pp. 155–196, 2005.

[11] H. Mohamed, "Use of microfluidic technology for cell separation," *blood*, vol. 1, pp. 3–3, 2012, online; accessed 04-December-2015, http://cdn.intechopen.com/pdfs-wm/39119.pdf.

[12] A. Sin, S. K. Murthy, A. Revzin, R. G. Tompkins, and M. Toner, "Enrichment using antibody-coated microfluidic chambers in shear flow: Model mixtures of human lymphocytes," *Biotechnology and Bioengineering*, vol. 91, no. 7, pp. 816–826, 2005.

[13] A. Y. Fu, H.-P. Chou, C. Spence, F. H. Arnold, and S. R. Quake, "An integrated microfabricated cell sorter," *Analytical Chemistry*, vol. 74, no. 11, pp. 2451–2457, 2002.

[14] A. Revzin, K. Sekine, A. Sin, R. G. Tompkins, and M. Toner, "Development of a microfabricated cytometry platform for characterization and sorting of individual leukocytes," *Lab on a Chip*, vol. 5, no. 1, pp. 30–37, 2005.

[15] D. R. Gossett, W. M. Weaver, A. J. Mach, S. C. Hur, H. T. K. Tse, W. Lee, H. Amini, and D. Di Carlo, "Label-free cell separation and sorting in microfluidic systems," *Analytical and Bioanalytical Chemistry*, vol. 397, no. 8, pp. 3249–3267, 2010.

[16] H. M. Ji, V. Samper, Y. Chen, C. K. Heng, T. M. Lim, and L. Yobas, "Silicon-based microfilters for whole blood cell separation," *Biomedical microdevices*, vol. 10, no. 2, pp. 251–257, 2008.

[17] M. Yamada, M. Nakashima, and M. Seki, "Pinched flow fractionation: continuous size separation of particles utilizing a laminar flow profile in a pinched microchannel," *Analytical Chemistry*, vol. 76, no. 18, pp. 5465–5471, 2004.

[18] L. R. Huang, E. C. Cox, R. H. Austin, and J. C. Sturm, "Continuous particle separation through deterministic lateral displacement," *Science*, vol. 304, no. 5673, pp. 987–990, 2004.

[19] D. W. Inglis, J. A. Davis, R. H. Austin, and J. C. Sturm, "Critical particle size for fractionation by deterministic lateral displacement," *Lab on a Chip*, vol. 6, no. 5, pp. 655–658, 2006.

[20] J. C. Giddings, "Field-flow fractionation: analysis of macromolecular, colloidal, and particulate materials," *Science*, vol. 260, no. 5113, pp. 1456–1465, 1993.

[21] S. Choi and J.-K. Park, "Continuous hydrophoretic separation and sizing of microparticles using slanted obstacles in a microchannel," *Lab on a Chip*, vol. 7, no. 7, pp. 890–897, 2007.

[22] J. Seo, M. H. Lean, and A. Kole, "Membrane-free microfiltration by asymmetric inertial migration," *Applied Physics Letters*, vol. 91, no. 3, pp. 033 901–033 901, 2007.

[23] D. Huh, J. H. Bahng, Y. Ling, H.-H. Wei, O. D. Kripfgans, J. B. Fowlkes, J. B. Grotberg, and S. Takayama, "Gravity-driven microfluidic particle sorting device with hydrodynamic separation amplification," *Analytical Chemistry*, vol. 79, no. 4, pp. 1369–1376, 2007.

[24] S. S. Shevkoplyas, T. Yoshida, L. L. Munn, and M. W. Bitensky, "Biomimetic autoseparation of leukocytes from whole blood in a microfluidic device," *Analytical Chemistry*, vol. 77, no. 3, pp. 933–937, 2005.

[25] S. Yang, A. Ündar, and J. D. Zahn, "A microfluidic device for continuous, real time blood plasma separation," *Lab on a Chip*, vol. 6, no. 7, pp. 871–880, 2006.

[26] E. Furlani, "Magnetophoretic separation of blood cells at the microscale," *Journal of Physics D: Applied Physics*, vol. 40, no. 5, pp. 1313–1313, 2007.

[27] J. R. SooHoo and G. M. Walker, "Microfluidic aqueous two phase system for leukocyte concentration from whole blood," *Biomedical Microdevices*, vol. 11, no. 2, pp. 323–329, 2009.

[28] T. Laurell, F. Petersson, and A. Nilsson, "Chip integrated strategies for acoustic separation and manipulation of cells and particles," *Chemical Society Reviews*, vol. 36, no. 3, pp. 492–506, 2007.

[29] F. Petersson, L. Åberg, A.-M. Swärd-Nilsson, and T. Laurell, "Free flow acoustophoresis: microfluidic-based mode of particle and cell separation," *Analytical chemistry*, vol. 79, no. 14, pp. 5117–5123, 2007.

[30] M. D. Vahey and J. Voldman, "An equilibrium method for continuous-flow cell sorting using dielectrophoresis," *Analytical Chemistry*, vol. 80, no. 9, pp. 3135–3143, 2008.

[31] T. D. Chung and H. C. Kim, "Recent advances in miniaturized microfluidic flow cytometry for clinical use," *Electrophoresis*, vol. 28, no. 24, pp. 4511–4520, 2007.

[32] M. Nadi and F. Jaspard, "Dielectric properties of blood: an investigation of haematocrit dependance," *Physiological Measurement*, vol. 24, no. 17, pp. 137–147, 2003.

[33] T. F. for Research on Information Technologies in Society (IT'IS), "*'is database — thermal tissue properties — dielectric tissue properties— thermal and dielectric properties — low-frequency conductivity — documentation,"* 01.09.2015, online; accessed 04-December-2015, http://www.itis.ethz.ch/virtual-population/tissue-properties/database/database-summary.*

[34] *H. F. Acevedo, "Human chorionic gonadotropin (hcg), the hormone of life and death: a review,"* Journal of Experimental Therapeutics and Oncology*, vol. 2, no. 3, pp. 133–145, 2002.*

[35] *H. F. Acevedo, M. Pardo, E. Campbell-Acevedo, and G. J. Domingue, "Human choriogonadotropin-like material in bacteria of different species: electron microscopy and immunocytochemical studies with monoclonal and polyclonal antibodies,"* Journal of General Microbiology*, vol. 133, no. 3, pp. 783–791, 1987.*

[36] *H. F. Acevedo, J. Y. Tong, and R. J. Hartsock, "Human chorionic gonadotropin-beta subunit gene expression in cultured human fetal and cancer cells of different types and origins,"* Cancer*, vol. 76, no. 8, pp. 1467–1475, 1995.*

[37] *N. Garralda, I. Llatser, A. Cabellos-Aparicio, E. Alarcón, and M. Pierobon, "Diffusion-based physical channel identification in molecular nanonetworks,"* Nano Communication Networks*, vol. 2, no. 4, pp. 196–204, 2011.*

[38] *D. J. Aidley and P. R. Stanfield,* Ion channels: molecules in action. *Cambridge University Press, 1996.*

[39] *A. Alexander, "The healthy cell: Its structure and functions that are so essential to disease prevention and treatment,"* INI Newsletter June*, 1997.*

[40] W. Adey, S. Bawin, C. Byus, C. Cain, S. Lin-Liu, R. Luben, D. Lyle, P. Sagan, A. Sheppard, and M. Stell, "Tissue interactions with nonionizing electromagnetic fields. final report, march 1979-february 1986," Jerry L. Pettis Memorial Veterans Administration Medical Center, Loma Linda, CA (USA); Loma Linda Univ., CA (USA); California Univ., Riverside (USA). Div. of Biomedical Sciences, Tech. Rep., 1986.

[41] W. Adey, "Physiological signalling across cell membranes and cooperative influences of extremely low frequency electromagnetic fields," in Biological Coherence and Response to External Stimuli. Springer, 1988, pp. 148–170.

[42] A. Alexander, "Calcium 2-aep and calcium orotate found essential in the prevention and treatment of osteoporosis," INI Newsletter June, 1997.

[43] A. James, E. Ambrose, and J. Lowick, "Differences between the electrical charge carried by normal and homologous tumour cells." Nature, vol. 177, no. 4508, pp. 576–577, 1956.

[44] L. Pauling and C. D. Coryell, "The magnetic properties and structure of the hemochromogens and related substances," Proceedings of the National Academy of Sciences of the United States of America, vol. 22, no. 3, pp. 159–159, 1936.

[45] K. R. Davey, C. H. Cheng, and C. M. Epstein, "Prediction of magnetically induced electric fields in biological tissue," IEEE Transactions on Biomedical Engineering, vol. 38, no. 5, pp. 418–422, 1991.

APPENDIX

APPENDIX: CONTACT INFORMATION

For simulation materials and models contact:

A) Department of Electrial and Computer Engineering,

Purdue School of Engineering,

Indiana University Purdue University Indianapolis,

723 W Michigan Street, SL 160, Indianapolis, IN, 46202

Phone: (317)274-9726.

B) Dr. Maher Rizkalla, P.E, Ph.D,

Email: mrizkall[at]iupui[dot]edu,

Department of Electrial and Computer Engineering,

Purdue School of Engineering,

Indiana University Purdue University Indianapolis,IN.

C) Vinaykumar Suryadevara, MSECE,

Email: vinaykumar.suryadevara[at]gmail[dotcom,

Department of Electrial and Computer Engineering,

Purdue School of Engineering,

Indiana University Purdue University Indianapolis,IN.